VISCOSITY OF LIQUID MIXTURES

By

THOMAS ELLIOTT TAYLOR

A DISSERTATION PRESENTED TO THE GRADUATE COUNCIL OF
THE UNIVERSITY OF FLORIDA
IN PARTIAL FULFILLMENT OF THE REQUIREMENTS FOR THE
DEGREE OF DOCTOR OF PHILOSOPHY

UNIVERSITY OF FLORIDA

April, 1967

ACKNOWLEDGMENTS

The writer wishes to express his sincere gratitude to Dr. T. M. Reed, III, who proposed and directed this work and who has constantly been a source of inspiration to him.

He also wishes to express his thanks to the National Science Foundation for both their support of research at the beginning of this work and for a Science Faculty Fellowship which permitted him to conclude his studies.

Finally, he wishes to thank his wife, Sandra, and all of their children for their loyal support and encouragement during a time that they were too often neglected by their husband and father.

TABLE OF CONTENTS

		Page
ACKNOWLEDGMENTS		ii
LIST OF TABLES		v
LIST OF FIGURES		vii
I.	INTRODUCTION	1
II.	APPARATUS	3
	Density	3
	Viscosity	3
	Temperature	3
	Vapor Pressure	4
	Refractive Index	4
	Vapor Chromatograms	4
	Surface Tensions	4
III.	MATERIALS	6
	Perfluoroheptane, C_7F_{16}	6
	Perfluorocyclic Ether, $C_8F_{16}O$	7
	2,2,3 Trichloroheptafluorobutane, $C_4Cl_3F_7$ and 1,2-Dichlorohexafluorocyclopentene-1, $C_5Cl_2F_6$	8
	n-Hexane, n-C_6H_{14}	8
	Isooctane, 2,2,4-Trimethylpentane, i-C_8H_{18}	9
IV.	EXPERIMENTAL RESULTS	12
	Viscosity Data	12
	Surface Tension Data	35
	Relative Surface Tensions by a Differential Capillary Rise Method	44
	Liquid Rise on Glass Walls	46

TABLE OF CONTENTS (Continued)

		Page
V.	CALCULATIONS FROM VISCOSITIES OF BINARY SYSTEMS	47
	Free Energy of Activation for Viscous Flow	47
	The Factor λ/a as a Variable	57
	Classification of Viscosity of Solutions	60
	Treatment of Class 3 Solutions	61
	Treatment of Class 2 Solutions	68
VI.	EXAMINATION OF THEORIES OF LIQUID VISCOSITY	70
	Temperature Dependence of Viscosity	70
	Corresponding States for Pure Materials	77
	Corresponding States for Binary Mixtures	82
VII.	CONCLUSIONS	88
BIBLIOGRAPHY		91
BIOGRAPHICAL SKETCH		96

LIST OF TABLES

Table		Page
1.	Physical Properties of Compounds Used in Experimental Work	10
2.	Systems Used in Experimental Work	23
3.	Density, Volume Change on Mixing and Refractive Indices for C_7F_{16} - $C_8F_{16}O$ System	25
4.	Density, Volume Change on Mixing and Refractive Indices for $C_5Cl_2F_6$ - $C_4Cl_3F_7$ System	26
5.	Density, Volume Change on Mixing and Refractive Indices for $C_4Cl_3F_7$ - $C_8F_{16}O$ System	27
6.	Density, Volume Change on Mixing and Refractive Indices for $C_5Cl_2F_6$ - $C_8F_{16}O$ System	28
7.	Density, Volume Change on Mixing and Refractive Indices for $C_5Cl_2F_6$ - C_7F_{16} System	29
8.	Density, Volume Change on Mixing and Refractive Indices for $\underline{n}$-C_6H_{14} - $C_5Cl_2F_6$ System	30
9.	Density, Volume Change on Mixing and Refractive Indices for $C_5Cl_2F_6$ - $\underline{i}$-C_8H_{18} System	31
10.	Density, Volume Change on Mixing and Refractive Indices for $\underline{i}$-C_8H_{18} - $C_8F_{16}O$ System	32
11.	Density, Volume Change on Mixing and Refractive Indices for $\underline{n}$-C_6H_{14} - $C_8F_{16}O$ System	33
12.	Density, Volume Change on Mixing and Refractive Indices for $\underline{i}$-C_8H_{18} - C_7F_{16} System	34
13.	Shape Factors for the $\underline{i}$-C_8H_{18} - $C_8F_{16}O$ and $\underline{i}$-C_8H_{18} - C_7F_{16} Systems	66

LIST OF TABLES (Continued)

Table		Page
14.	Shape Factors at the Critical Composition for the $\underline{i}$-C_8H_{18} - C_7F_{16} System	67
15.	Sources of Data for 52 Liquids Used to Test Viscosity Theories	71
16.	Liquid Density Parameters A and B from Equation 27	79

LIST OF FIGURES

Figure		Page
1.	Viscosities of the C_7F_{16} - $C_8F_{16}O$ System	13
2.	Viscosities of the $C_5Cl_2F_6$ - $C_4Cl_3F_7$ System	14
3.	Viscosities of the $C_4Cl_3F_7$ - $C_8F_{16}O$ System	15
4.	Viscosities of the $C_5Cl_2F_6$ - $C_8F_{16}O$ System	16
5.	Viscosities of the $C_5Cl_2F_6$ - C_7F_{16} System	17
6.	Viscosities of the n-C_6H_{14} - $C_5Cl_2F_6$ System	18
7.	Viscosities of the $C_5Cl_2F_6$ - i-C_8H_{18} System	19
8.	Viscosities of the i-C_8H_{18} - $C_8F_{16}O$ System	20
9.	Viscosities of the n-C_6H_{14} - $C_8F_{16}O$ System	21
10.	Viscosities of the i-C_8H_{18} - C_7F_{16} System	22
11.	Surface Tensions of the C_7F_{16} - $C_8F_{16}O$ System	36
12.	Surface Tensions of the $C_5Cl_2F_6$ - $C_4Cl_3F_7$ System	37
13.	Surface Tensions of the $C_4Cl_3F_7$ - $C_8F_{16}O$ System	38
14.	Surface Tensions of the n-C_6H_{14} - $C_5Cl_2F_6$ System	39
15.	Surface Tensions of the $C_5Cl_2F_6$ - i-C_8H_{18} System	40
16.	Surface Tensions of the i-C_8H_{18} - $C_8F_{16}O$ System	41
17.	Surface Tensions of the n-C_6H_{14} - $C_8F_{16}O$ System	42
18.	Surface Tensions of the i-C_8H_{18} - C_7F_{16} System	43

LIST OF FIGURES (Continued)

Figure		Page
19.	Excess Free Energies of Activation for the C_7F_{16} - $C_8F_{16}O$ System	49
20.	Excess Free Energies of Activation for the $C_5Cl_2F_6$ - $C_4Cl_3F_7$ System	49
21.	Excess Free Energies of Activation for the $C_4Cl_3F_7$ - $C_8F_{16}O$ System	50
22.	Excess Free Energies of Activation for the $C_5Cl_2F_6$ - $C_8F_{16}O$ System	50
23.	Excess Free Energies of Activation for the $C_5Cl_2F_6$ - C_7F_{16} System	51
24.	Excess Free Energies of Activation for the $\underline{n}$-C_6H_{14} - $C_5Cl_2F_6$ System	51
25.	Excess Free Energies of Activation for the $C_5Cl_2F_6$ - $\underline{i}$-C_8H_{18} System	51
26.	Excess Free Energies of Activation for the $\underline{i}$-C_8H_{18} - $C_8F_{16}O$ System	52
27.	Excess Free Energies of Activation for the $\underline{n}$-C_6H_{14} - $C_8F_{16}O$ System	52
28.	Excess Free Energies of Activation for the $\underline{i}$-C_8H_{18} - C_7F_{16} System	53
29.	Excess Free Energy as a Function of Volume Change on Mixing	55
30.	$R\ \partial \ln \mu / \partial(1/T)$ as a Function of Temperature for the $\underline{i}$-C_8H_{18} - C_7F_{16} System	58
31.	Excess Free Energy Function for the $\underline{i}$-C_8H_{18} - C_7F_{16} System	64
32.	Excess Free Energy Function for the $\underline{i}$-C_8H_{18} - $C_8F_{16}O$ System	65

LIST OF FIGURES (Continued)

Figure		Page
33.	Reduced Relationship for "a" of Equation 43	84
34.	Reduced Relationship for "b" of Equation 43	85

I. INTRODUCTION

Although a great deal of progress has been made in describing the gaseous and solid states of matter, the situation with liquids is far from clear and highly disputed [42].[a] Of all the properties of liquids, viscosity has probably received the greatest attention [67]. The viscosity data that have been collected on mixtures, however, usually have not covered both full composition ranges and a range of temperatures. The present work provides such data for a variety of systems that range from ideal solutions in the thermodynamic sense, to ones in which two liquid phases are formed. Viscosity data at temperatures and compositions in the neighborhood of phase separation have been particularly lacking.

With the large amounts of data available, numerous attempts have been made to develop theories of viscosity. These theories have been collected by Partington [71] and, more recently, in a thorough review by Brush [15]. In many of these cases the theories have been developed using the data for only a few compounds. This suggested that a further examination should be made to determine which of these theories are simply empirical fits of data and which offer a reasonable description of the liquid state on the molecular level.

---

[a] Numbers in square brackets [ ] refer to references in the Bibliography.

In the present work some of the factors involved in flow have been separated. These include a volume factor and a local inhomogeniety factor. It is also proposed that the interaction between rigid acentric molecules affects the molecular rotational motion. This effect is accompanied by a rotational energy of activation for viscous flow. This may explain many of the viscosities and the temperature coefficients of viscosity which deviate widely from current theories.

Some preliminary work on surface tensions has been done and a unique observation, that of liquids rising in a thin film as much as 8 cm. on a glass wall, has been noted for certain hydrocarbon-fluorocarbon mixtures.

II. APPARATUS

Density. Pycnometers described by Lipkin [57] were calibrated with distilled mercury at each temperature for which liquid densities were determined. The nominal capacity of the pycnometers was 1 milliliter and 10 milliliters. The precision of the density values obtained is ± 0.0002 grams per milliliter in the one-milliliter pycnometers.

Viscosity. The Cannon-Fenske modification [5] of the Ostwald viscometer was calibrated with an oil of standard viscosity obtained from the National Bureau of Standards and with a sample of pure toluene. The physical properties of the toluene (density, boiling point, and refractive index) were identical with those given in "Selected Values of Physical and Thermodynamic Properties of Hydrocarbons," published by Project 44 of the American Petroleum Institute at the Carnegie Institute of Technology. The viscometers were calibrated at each temperature for which viscosities were determined. Ubbelohde suspended level viscometers [5] calibrated by the Cannon Instrument Company were used for about 60 per cent of the measurements and reproduced the data obtained with the other viscometers. The clocks were calibrated with reference to the standard time intervals transmitted by radio station WWV. The precision of the viscosities is 2 parts in 1000.

Temperature. All mercury-in-glass thermometers and all thermocouples used in measuring thermostat temperatures and boiling temperatures (except those reported in distillations) were calibrated against

an iron-constantan thermocouple calibrated at the National Bureau of Standards. The accuracy of the standard thermocouple was ± 0.01°C.

Vapor Pressure. The vapor pressure-temperature determinations on the pure materials were obtained by boiling the liquid in a Cottrel apparatus under a measured air pressure. The boiling temperatures were obtained from calibrated thermocouples. The pressure was measured with a precision of ± 0.05 mm. Hg with a one-meter cathotometer and a mercury column 20 mm. in diameter.

Refractive Index. Abbe-type instruments were used for these measurements. One refractometer had a range of 1.2 to 1.4 while the other had the standard range of 1.3 to 1.6.

Vapor Chromatograms. A Perkin-Elmer Model 154 "Vapor Fractometer" was used for the chromatographic determinations of purity. The carrier gases used were nitrogen and helium. The stationary media used to separate fluorocarbon materials were those reported [77] to be effective (e.g., $Cl(CF_2CFCl)_3CF_2COOC_2H_5$ and $(C_4F_9)_3N$).

Surface Tensions. The surface tensions were measured by a drop weight technique [93]. The apparatus consisted of a glass capillary tube with a tip which was machined to a circular diameter of 2.46 ± 0.01 mm. and polished flat. Drops were slowly formed on this tip (one to four minutes per drop) and allowed to fall into a small weighing bottle. The weighing bottle was located upon a small platform in an enclosure containing a sufficient amount of the liquid being tested to insure vapor saturation of the atmosphere.

Between ten and twenty drops were used in each determination and each of the determinations was duplicated. An average precision of approximately 1 per cent was obtained.

An apparatus has been designed which will give unusually high accuracy in measuring relative surface tensions although no measurements with this equipment are included in this work. This apparatus consists of a U tube in which one arm is a capillary and the other is a large precision bore glass tube. The large tube is equipped with a ground-glass cover to prevent evaporation of the liquid. Liquid of known density is admitted to the large tube until the liquid level in the capillary reaches an etched mark. The difference in weight of the apparatus before and after filling allows the capillary rise to be calibrated very accurately. Since each liquid is added until the level in the capillary has reached the same point, the effect of any irregularities in the bore or optical aberrations in the glass are eliminated.

III. MATERIALS

Perfluoroheptane, C_7F_{16}. A fluorocarbon sample (Minnesota Mining and Manufacturing Company material FM-3130) was shown by vapor chromatography to contain at least 19 components, the major component (approx. 73%) being C_7F_{16}. A charge of 1319 grams of this material was distilled in a column equal to 60 theoretical plates when distilling hydrocarbons.[a] The constant boiling center portion of the product, 659.2 grams, gave only two peaks upon analysis by vapor chromatography. The second peak constituted approximately 1 to 2 per cent of this material. This constant boiling material was then azeotroped with 198.7 grams of n-heptane in the 60-plate column. An improved material came overhead as the initial product in the form of an azeotrope boiling approximately 9°C below the flat obtained in the original distillation. The first 387.5 grams of this azeotrope were cooled to dry-ice temperature where the hydrocarbon and fluorocarbon are almost completely immiscible. The two layers were separated mechanically. This gave 356.4 grams of fluorocarbon-rich layer which was placed in a distillation column equal to 30 theoretical plates when distilling hydrocarbons.

---

[a] The distillation columns used in this work were packed with 1/16 inch single-turn helices. It has been shown [97] that such columns have about one-half as many theoretical plates when distilling fluorocarbons as when distilling hydrocarbons. The values quoted are for the number of theoretical plates in the columns when used for distilling hydrocarbons.

The remaining traces of dissolved n-heptane were then removed as the azeotrope. When analysis by vapor chromatography showed no more n-heptane in the overhead the distillation was stopped. The residue from this distillation (322.9 g.) was taken as the pure C_7F_{16} for the viscosity studies.

Under extremely high sensitivity on the vapor chromatograph, (helium carrier gas) this C_7F_{16} material showed a small shoulder on the back of the main peak. Since these two materials appear so close together it has been assumed that they are two different C_7F_{16} isomers. This is further borne out by the nuclear magnetic resonance spectrum run on another C_7F_{16} sample from the same source which gave an almost identical trace on the vapor chromatograph under the same high resolution.

The second component showed the presence of $(CF_3)_2C$ structure in an amount no greater than 10 per cent as a C_7F_{16} isomer. Askew [4] has identified this isomer as $2\text{-}CF_3C_6F_{13}$. The only other peaks in the nuclear magnetic resonance (n.m.r.) spectrum were those for $n\text{-}C_7F_{16}$.

This C_7F_{16} material has a boiling point of 82.3°C at 760 mm. Hg.

Perfluorocyclic Ether, $C_8F_{16}O$. Fractionation of 2951 grams of Minnesota Mining and Manufacturing Company Fluorochemical 101 in a 60-plate distillation column yielded 617.3 g. of material refluxing at 101°C with a refractive index of from $n^{25} = 1.2772$ to $n^{25} = 1.2774$. Vapor chromatography showed this material to contain one major component (95%) and three minor components. This material was then refluxed 77 hours with 80 g. of KOH to decompose any hydrogen-containing material. At the end of this time the KOH pellets had turned dark brown. The fluorocarbon was removed and again refluxed with 80 g. of fresh KOH

for 63 hours. At the end of this treatment the fluorocarbon was washed four times with equal volumes of distilled water, dried with $CaCl_2$, and simple distilled. This product had a refractive index of $n^{25} = 1.2775$. Vapor chromatography still indicated the presence of small amounts of three minor components. The 568 grams of material that remained from the above treatment was distilled in the 60-plate column with 127 g. of n-heptane. Most of the remaining impurities came overhead in a fraction refluxing at 82.1 to 83.9°C. These latter fractions were combined with the residue and cooled to dry-ice temperature. The bottom layer contained 429 g. This layer was distilled in a 30-plate column to remove the final traces of n-heptane as the azeotrope. The residue showed a small shoulder on the back of the main peak under high sensitivity in the vapor chromatograph. This impurity represents less than 1 per cent of the sample. This material was taken as the $C_8F_{16}O$ for the viscosity studies. It has a boiling point of 103.0°C at 760 mm. Hg.

$C_8F_{16}O$ is a cyclic perfluoro ether of unknown structure. It is believed that the oxygen atom is in the ring, however [66].

2,2,3-Trichloroheptafluorobutane, $C_4Cl_3F_7$ and 1,2-Dichlorohexafluorocyclopentene-1, $C_5Cl_2F_6$. These materials used in the viscosity studies were constant boiling fractions obtained from the distillations, in a 60-plate column, of two crude materials obtained from the Hooker Electrochemical Company. Vapor chromatography indicated only a very small amount of impurity (less than 0.5%) in both materials.

n-Hexane, n-C_6H_{14}. Commercial grade hexane was washed with H_2SO_4, passed through silica gel, and distilled in a 60-plate column. The fractions containing predominantly n-hexane were again washed with

H_2SO_4, and azeotroped with excess ethanol in the 60-plate column. The azeotrope was washed with water, dried, and the remaining ethanol removed as the azeotrope in a 30-plate column. The n-hexane used in these studies was a constant boiling fraction from this distillation in which no impurities were indicated by vapor chromatography.

Isooctane, 2,2,4-Trimethylpentane, i-C_8H_{18}. The isooctane used in these studies was Phillips 99 mole-per cent-minimum grade. Vapor chromatograms of this material showed no impurities.

The physical properties of these compounds are summarized in Table 1.

TABLE 1

Physical Properties of Compounds Used in Experimental Work

Compound	Formula	B.p., °C	ρ, density 25°C	$\frac{-d\rho}{dt}$, g./(ml.°C) X10^3	Vapor pressure constants[a] A	B	C
n-Hexane	n-C_6H_{14}	68.74	0.6550	0.91	...	...	...
2,2,4-Trimethyl-pentane	i-C_8H_{18}	99.24	0.6879	0.83	...	...	...
1,2-Dichloro-hexafluoro-cyclopentene	$C_5Cl_2F_6$	90.81	1.6433	2.18	6.78904	1163.9	207.00
2,2,3-Trichloro-heptafluoro-butane	$C_4Cl_3F_7$	97.51	1.7386	2.20	6.81718	1240.14	217.54
Perfluoroheptane	C_7F_{16}	82.26	1.7275	2.78	6.07134	771.4	159.52
Perfluorocyclic oxide	$C_8F_{16}O$	103.05	1.7640	2.58	6.98972	1284.6	209.59

[a] $\log_{10}P(\text{mm.}) = A - B/(C + t)$, t in °C.

TABLE 1 (Continued)

Formula	Refrac. index 25°C	Heat of vaporization, cal./mole, at 25°C	B.p.	Viscosity, 25°C cs.	cp.	$\frac{\partial \ln \mu}{\partial (1/T)}$, °K	$\frac{\Delta E_{vap}}{R \partial \ln \mu / \partial (1/T)}$ at 25°C	δ, 25°C (c) (cal./cc.)$^{1/2}$
n-C_6H_{14}	1.3723	7540(b)	6896	0.4468	0.2938	755	4.63	7.27
i-C_8H_{18}	1.3890	8396(b)	7410	0.6869	0.4725	910	4.31	6.85
$C_5Cl_2F_6$	1.3657	8730	7520	0.5528	0.9084	1070	3.83	7.39
$C_4Cl_3F_7$	1.3505	8510	7370	1.1271	1.9596	1640	2.43	6.92
C_7F_{16}	1.2599	8215	7195	0.5184	0.8955	1290	2.97	5.83
$C_8F_{16}O$	1.2772	9440	8040	0.7916	1.3964	1520	2.93	6.13

(b) Reference [1].

(c) $\delta = (\Delta E_{vap}/V)^{1/2}$.

IV. EXPERIMENTAL RESULTS

Viscosity Data. The viscosities have been studied for ten binary systems. Viscosities and densities were measured for eleven compositions in each system at 5°C intervals from 25°C to 45°C. The experimental kinematic viscosities are presented in Figures 1 through 10. These figures are all drawn to the same scale. The composition in each mixture is expressed in terms of the volume fraction at 25°C of the component with the greater kinematic viscosity as a pure compound.

This series of systems allows a systematic study to be made of solutions varying from the ideal to those with large positive deviations in the activity coefficient from the ideal solution behavior. These systems are listed in Table 2 in the order of increasing positive deviation from thermodynamically ideal behavior. The K values defined in this table are those which appear in Hildebrand's theory [41]. In this theory, the logarithm of the activity coefficient of compound "a" is $K_a\varphi_b^2/T$, where φ_b is the volume fraction of component b. K equals zero for an ideal solution and increases with larger deviations from the thermodynamic ideal solution behavior. Solutions of fluorocarbons with hydrocarbons require special treatment [76, 98]. The K values listed in Table 2 have been shown [98] to describe the activity coefficients of systems one through four fairly accurately. From Tables 3 through 12 it can be seen that the volume change on mixing increases rather steadily

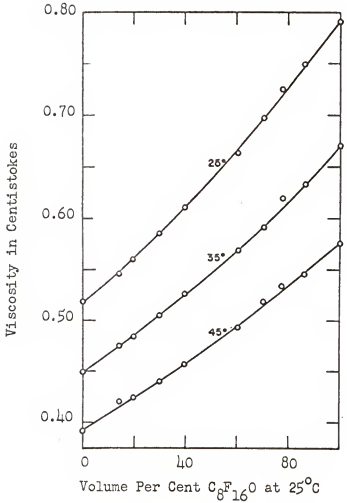

Figure 1.--Viscosities of the C_7F_{16} - $C_8F_{16}O$ System

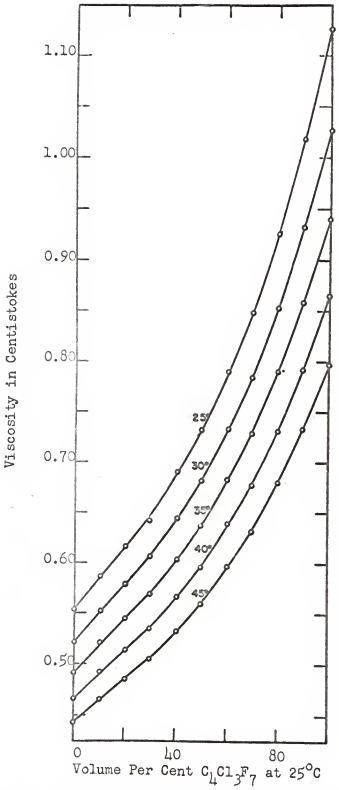

Figure 2.--Viscosities of the $C_5Cl_2F_6$ - $C_4Cl_3F_7$ System

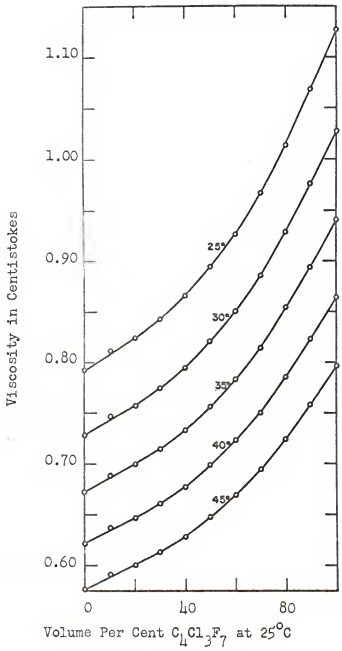

Figure 3.--Viscosities of the $C_4Cl_3F_7$ - $C_8F_{16}O$ System

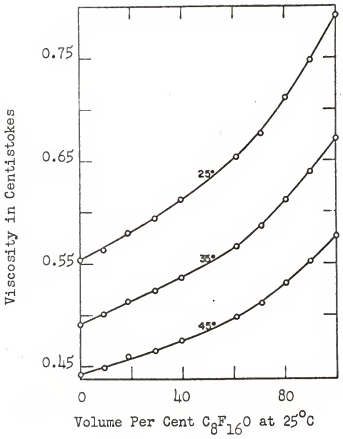

Figure 4.--Viscosities of the $C_5Cl_2F_6$ - $C_8F_{16}O$ System

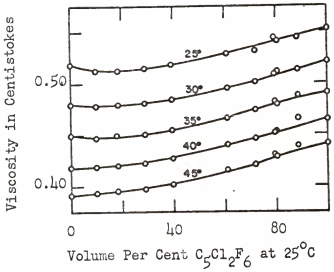

Figure 5.--Viscosities of the $C_5Cl_2F_6$ - C_7F_{16} System

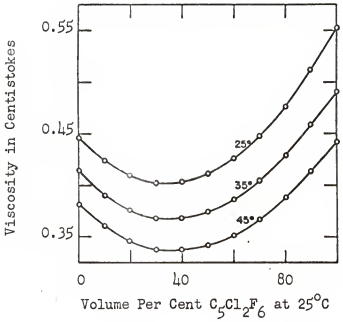

Figure 6.--Viscosities of the n-C_6H_{14} - $C_5Cl_2F_6$ System

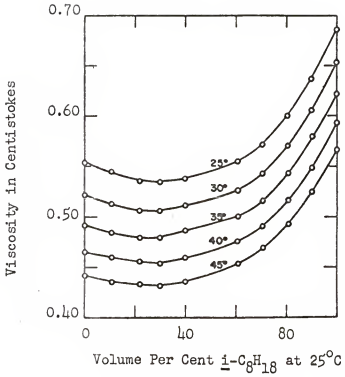

Figure 7.--Viscosities of the $C_5Cl_2F_6$ - i-C_8H_{18} System

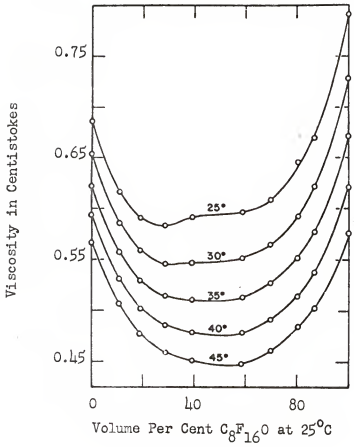

Figure 8.--Viscosities of the i-C_8H_{18} - $C_8F_{16}O$ System

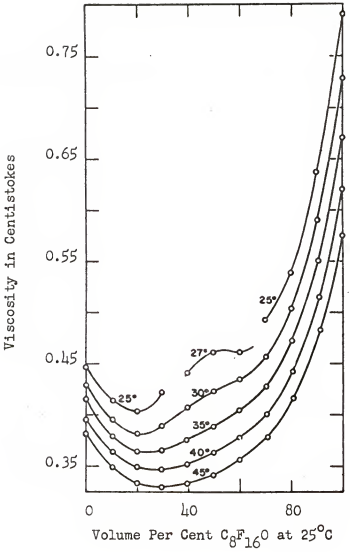

Figure 9.--Viscosities of the $\underline{n}$-C_6H_{14} - $C_8F_{16}O$ System

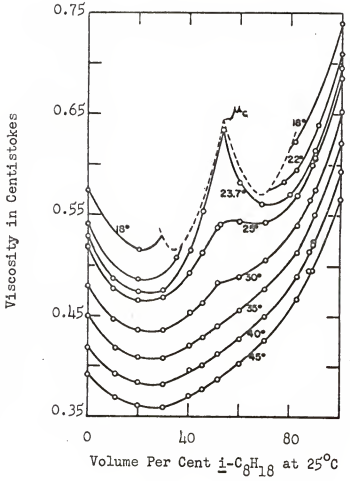

Figure 10.--Viscosities of the $\underline{i}$-C_8H_{18} - C_7F_{16} System

TABLE 2

Systems Used in Experimental Work

System		V_a/V_b	$\delta_a - \delta_b$, 25°C (cal./cc.)$^{1/2}$	K_a, °K
a	b			
1. C_7F_{16}:	$C_8F_{16}O$	0.960	0.30	1.0[a]
2. $C_5Cl_2F_6$:	$C_4Cl_3F_7$	0.904	0.47	16.6[a]
3. $C_4Cl_3F_7$:	$C_8F_{16}O$	0.702	0.79	52.0[a]
4. $C_5Cl_2F_6$:	$C_8F_{16}O$	0.634	1.26	119[a]
5. $C_5Cl_2F_6$:	C_7F_{16}	0.666	1.56	182[a]
6. n-C_6H_{14}:	$C_5Cl_2F_6$	0.882	0.12	213[b]
7. $C_5Cl_2F_6$:	i-C_8H_{18}	0.898	0.54	250[b]
8. i-C_8H_{18}:	$C_8F_{16}O$	0.706	0.72	254[b]
9. n-C_6H_{14}:	$C_8F_{16}O$	0.559	1.14	262[b]
10. i-C_8H_{18}:	C_7F_{16}	0.740	1.02	286[b]

(a) $K_a = (V_a/R)(\delta_a-\delta_b)^2$. (b) $K_a = (V_a/R)[(\delta_a-\delta_b)^2 + 0.06\ \delta_a\delta_b]$.

$\delta = (\Delta E_{vap}/V)^{1/2}$, solubility parameter [41].

from a very small negative value on the order of -0.01 per cent for system one, through larger positive values up to approximately 1 to 3 per cent of the total volume for system ten.

Vapor-liquid equilibrium data for systems one and two show that these components form solutions very close to ideal while system three is sufficiently non-ideal to form an azeotrope at atmospheric pressure [98]. Vapor-liquid equilibrium data are not available for system five, but for system four positive deviations from Raoult's law are known. Systems five, six and seven are shown to be less ideal than those of the chlorofluorocarbons with fluorocarbons by the K-values of Table 2. (It is known that $C_4Cl_3F_7$ forms a minimum boiling azeotrope with n-heptane at atmospheric pressure [98].) No thermodynamic data are available for system eight, but like all fluorocarbon-hydrocarbon solutions this one undoubtedly has large activity coefficients.

No thermodynamic data are available for system nine. The critical unmixing temperature was determined in this work at 26°C at 27 mole per cent $C_8F_{16}O$.

For system ten, both vapor-liquid [69] and liquid-liquid [40] data are available. The kinematic viscosity of this system (Figure 10) has been examined in greater detail than that of the above systems. As the temperature is decreased from 45°C to 25°C, the portion of the curve in the middle composition range becomes at first linear at 35°C, and then exhibits a slight rise at 30°C which finally becomes a maximum at 25°C. The critical unmixing temperature for this system has been observed variously at 23.7°C in reference [40] (for n-C_7F_{16}) and at 23.65°C in this work for the C_7F_{16} material used. The dashed line

TABLE 3

Density, Volume Change on Mixing and Refractive Indices for C_7F_{16} - $C_8F_{16}O$ System

System 1

Volume[a] % C_7F_{16} at 25°C	Mole % C_7F_{16}	Refrac. index, 25°C	ρ, Density g/ml., 25°C	$\frac{-d\rho}{dT}$ X10^3 g/ml.°C	ΔV mixing, ml./mole 25°C	45°C
10.00	10.45	1.2758	1.7605	2.60	-0.020	-0.043
20.00	20.79	1.2740	1.7571	2.63	-0.054	-0.057
30.00	31.03	1.2721	1.7536	2.65	-0.074	-0.085
40.00	41.18	1.2703	1.7500	2.67	-0.081	-0.098
50.00	51.22	1.2686	1.7464	2.69	-0.088	-0.111
60.00	61.16	1.2669	1.7428	2.71	-0.094	-0.122
70.00	71.01	1.2652	1.7390	2.73	-0.075	-0.106
80.00	80.77	1.2636	1.7352	2.75	-0.055	-0.077
90.00	90.43	1.2618	1.7313	2.78	-0.023	-0.032

[a] Assuming no volume change on mixing.

TABLE 4

Density, Volume Change on Mixing and Refractive Indices for $C_5Cl_2F_6$ - $C_4Cl_3F_7$ System

System 2

Volume[a] % $C_5Cl_2F_6$ at 25°C	Mole % $C_5Cl_2F_6$	Refrac. index, 25°C	ρ, Density g./ml., 25°C	$\frac{-d\rho}{dT}$ X10^3 g./ml.°C	ΔV mixing, ml./mole 25°C	45°C
10.22	11.22	1.3521	1.7286	2.20	+0.02	+0.02
20.00	21.71	1.3535	1.7192	2.20	0.03	0.04
30.06	32.28	1.3549	1.7095	2.20	0.05	0.06
39.85	42.36	1.3563	1.7001	2.20	0.04	0.07
50.16	52.74	1.3580	1.6905	2.20	0.03	0.08
59.66	62.12	1.3594	1.6813	2.20	0.05	0.07
70.22	72.34	1.3611	1.6714	2.20	0.03	0.06
80.02	81.62	1.3626	1.6622	2.20	0.01	0.05
89.92	90.81	1.3643	1.6527	2.20	0.02	0.07

[a] Assuming no volume change on mixing.

TABLE 5

Density, Volume Change on Mixing and Refractive Indices for $C_4Cl_3F_7$ - $C_8F_{16}O$ System

System 3

Volume[a] % $C_4Cl_3F_7$ at 25°C	Mole % $C_4Cl_3F_7$	Refrac. index, 25°C	ρ, Density g./ml., 25°C	$\frac{-d\rho}{dT}$ X10^3 g./ml.°C	ΔV mixing, ml./mole 25°C	45°C
10.30	14.07	1.2841	1.7582	2.55	+0.41	+0.48
20.14	26.46	1.2908	1.7533	2.51	0.69	0.74
20.93	37.87	1.2977	1.7494	2.48	0.83	0.91
39.94	48.68	1.3046	1.7462	2.44	0.88	0.96
49.77	58.57	1.3117	1.7437	2.40	1.09	1.17
59.98	68.14	1.3192	1.7416	2.36	0.77	0.83
70.01	76.91	1.3268	1.7400	2.32	0.65	0.69
79.93	85.02	1.3345	1.7391	2.28	0.46	0.50
89.70	92.55	1.3423	1.7386	2.24	0.25	0.27

[a] Assuming no volume change on mixing.

TABLE 6

Density, Volume Change on Mixing and Refractive Indices for $C_5Cl_2F_6$ - $C_8F_{16}O$ System

System 4

Volume[a] % $C_5Cl_2F_6$ at 25°C	Mole % $C_5Cl_2F_6$	Refrac. index, 25°C	ρ, Density, g./ml., 25°C	$\frac{-d\rho}{dT}$ X10^3 g./ml.°C	ΔV mixing, ml./mole 25°C	45°C
10.00	14.95	1.2851	1.7483	2.55	+0.46	+0.51
20.00	28.35	1.2933	1.7339	2.52	0.73	0.82
30.00	40.41	1.3018	1.7201	2.49	0.86	0.98
40.00	51.34	1.3107	1.7075	2.45	0.92	1.05
50.00	61.28	1.3197	1.6955	2.40	0.88	1.00
60.00	70.36	1.3285	1.6839	2.37	0.80	0.92
70.00	78.69	1.3374	1.6730	2.34	0.65	0.78
80.00	86.36	1.3466	1.6628	2.28	0.45	0.53
90.00	93.46	1.2560	1.6529	2.23	0.23	0.28

[a] Assuming no volume change on mixing.

TABLE 7

Density, Volume Change on Mixing and Refractive Indices for $C_5Cl_2F_6$ - C_7F_{16} System

System 5

Volume[a] % $C_5Cl_2F_6$ at 25°C	Mole % $C_5Cl_2F_6$	Refrac. index, 25°C	ρ, Density g./ml., 25°C	$\frac{-d\rho}{dT}$ X10^3 g./ml.°C	ΔV mixing, ml./mole 25°C	45°C
10.00	15.34	1.2697	1.7158	2.75	+0.41	+0.48
20.00	27.37	1.2798	1.7051	2.69	0.66	0.76
30.00	39.24	1.2901	1.6956	2.68	0.76	0.86
40.00	50.12	1.3005	1.6869	2.59	0.76	0.90
50.00	60.11	1.3111	1.6783	2.51	0.76	0.87
60.00	69.33	1.3217	1.6705	2.45	0.67	0.77
70.00	77.86	1.3326	1.6629	2.36	0.56	0.61
80.00	85.77	1.3435	1.6560	2.29	0.40	0.41
90.00	93.13	1.3545	1.6495	2.23	0.21	0.21

[a] Assuming no volume change on mixing.

TABLE 8

Density, Volume Change on Mixing and Refractive Indices for $\underline{n}$-C_6H_{14} - $C_7Cl_2F_6$ System

System 6

Volume[a] % $\underline{n}$-C_6H_{14} at 25°C	Mole % $\underline{n}$-C_6H_{14}	Refrac. index, 25°C	ρ, Density g./ml.,25°C	$\frac{-d\rho}{dT}$ X10^3 g./ml.°C	ΔV mixing, ml./mole 25°C	45°C
10.12	11.30	1.3648	1.5394	2.10	+0.38	+0.52
19.84	21.90	1.3642	1.4368	1.99	1.05	1.25
30.05	32.74	1.3640	1.3338	1.87	1.35	1.60
39.81	42.81	1.3640	1.2400	1.75	1.12	1.37
50.05	53.17	1.3645	1.1388	1.60	1.21	1.44
60.22	63.17	1.3652	....	...	....	....
70.08	72.63	1.3663	0.9422	1.35	1.23	1.52
80.31	82.21	1.3680	0.8435	1.20	0.98	1.21
90.00	91.07	1.3700	0.7521	0.89	0.31	-0.14

[a] Assuming no volume change on mixing.

TABLE 9

Density, Volume Change on Mixing and Refractive Indices for $C_5Cl_2F_6$ - i-C_8H_{18} System

System 7

Volume[a] % $C_5Cl_2F_6$ at 25°C	Mole % $C_5Cl_2F_6$	Refrac. index 25°C	ρ, Density g./ml., 25°C	$\frac{-d\rho}{dT}$ X10^3 g./ml.°C	ΔV mixing, ml./mole 25°C	45°C
10.00	11.01	1.3850	0.7803	0.96	+0.66	+0.72
20.00	21.78	1.3816	0.8741	1.08	0.91	0.95
30.00	32.31	1.3787	0.9670	1.16	1.25	1.21
40.00	42.61	1.3761	1.0630	1.39	1.05	1.25
50.00	52.69	1.3737	1.1555	1.42	1.37	1.28
60.00	62.55	1.3715	1.2506	1.51	1.31	1.12
70.00	72.21	1.3696	1.3470	1.66	1.11	0.94
80.00	81.67	1.3680	1.4464	1.80	0.61	0.78
90.00	90.93	1.3667	1.5453	2.13	0.24	0.47

[a] Assuming no volume change on mixing.

TABLE 10

Density, Volume Change on Mixing and Refractive Indices for $\underline{i}$-C_8H_{18} - $C_8F_{16}O$ System

System 8

Volume[a] % $\underline{i}$-C_8H_{18} at 25°C	Mole % $\underline{i}$-C_8H_{18}	Refrac. index, 25°C	ρ, Density g./ml.,25°C	$\frac{-d\rho}{dT}$ X10^3 g./ml.°C	ΔV mixing, ml./mole 25°C	45°C
10.00	13.63	1.2850	1.6441	2.60	+1.69	+2.44
20.00	26.21	1.2931	1.5274	2.56	3.05	4.37
30.00	37.84	1.3019	1.4135	2.28	4.10	5.24
40.00	48.64	1.3120	1.3059	2.13	4.28	5.56
50.00	58.69	1.3233	1.1990	1.88	4.38	5.46
60.00	68.06	1.3350	1.0928	1.63	4.40	5.24
70.00	76.83	1.2473	0.9895	1.40	3.91	4.53
80.00	85.04	1.3601	0.8875	1.11	3.11	3.16
90.00	92.75	1.3739	0.7888	1.00	1.45	1.62

[a] Assuming no volume change on mixing.

TABLE 11

Density, Volume Change on Mixing and Refractive Indices for $\underline{n}$-C_6H_{14} - $C_8F_{16}O$ System

System 9

Volume[a] % $\underline{n}$-C_6H_{14} at 25°C	Mole % $\underline{n}$-C_6H_{14}	Refrac. index, 25°C	ρ, Density g./ml., 25°C	$\frac{-d\rho}{dT}$ X10^3 g./ml.°C	ΔV mixing, ml./mole 25°C	ΔV mixing, ml./mole 45°C
10.06	16.71	1.2823	1.6310	2.47	+2.86	+3.23
20.00	30.93	1.2889	1.5225	2.38	2.65	3.26
29.96	43.41	1.2965	1.4085	2.28	3.14	4.00
40.03	54.49	Two Liquid Phases				
50.15	64.32					
60.16	73.03					
70.35	80.96	1.3352	0.9643	1.55	3.08	3.92
80.04	87.79	1.3460	0.8596	1.30	2.78	3.33
89.74	94.01	1.3580	0.7603	1.10	1.52	1.84

[a] Assuming no volume change on mixing.

TABLE 12

Density, Volume Change on Mixing and Refractive Indices for $\underline{i}$-C_8H_{18} - C_7F_{16} System

System 10

Volume[a] % $\underline{i}$-C_8H_{18} at 25°C	Mole % $\underline{i}$-C_8H_{16}	Refrac. index, 25°C	ρ, Density g./ml.,25°C	$\frac{-d\rho}{dT}$ X10^3 g./ml.°C	ΔV mixing, ml./mole 25°C	45°C
10.00	13.07	1.2671	1.6098	2.84	+1.85	+2.76
20.00	25.27	1.2785	1.4979	2.68	3.03	4.27
30.00	36.70	1.2900	1.3880	2.40	4.04	5.18
40.00	47.42	1.3025	1.2804	2.12	4.80	5.79
50.00	57.50	1.3155	1.1747	1.82	5.36	6.08
60.00	66.99	1.3290	1.0735	1.62	5.40	5.92
70.00	75.94	1.3424	0.9770	1.37	4.20	4.59
80.00	84.40	1.3568	0.8802	1.20	3.11	3.44
90.00	92.41	1.3719	0.7841	1.00	1.69	1.83

[a] Assuming no volume change on mixing.

on Figure 10 is a portion of the approximate locus of the viscosities corresponding to the consolute curve. μ_c is the viscosity at the critical temperature of 23.65°C.

The isotherms of viscosity versus composition for system ten (Figure 10) are similar to those of system nine near the unmixing curve. The viscosities of systems eight, nine, and ten reveal that changes in the structure of the solution which ultimately produce separation into two equilibrium phases begin at temperatures at least 10C° above the temperature at which two liquid phases are observed.

Surface Tension Data. Surface tensions were determined for eight of the binary systems (all except systems four and five). The values for each system were obtained at three different temperatures (25°C, 35°C and 45°C) and at six compositions. These data are presented in Figures 11 through 18.

The deviations from linearity in volume fraction is seen to parallel closely the deviations from linearity of the kinematic viscosities for the same systems. Although these surface tension values are not extremely accurate (deviations up to 3 per cent from reported [1] values) the departure from linearity is well established. No further attempts were made to correlate the surface tensions with the viscosities when it was observed that neither the magnitude nor the temperature coefficient of surface tension paralleled the corresponding viscosity values for the pure components. It should be noted, however, that any adequate theory of the liquid mixtures should explain both surface tension and viscosity.

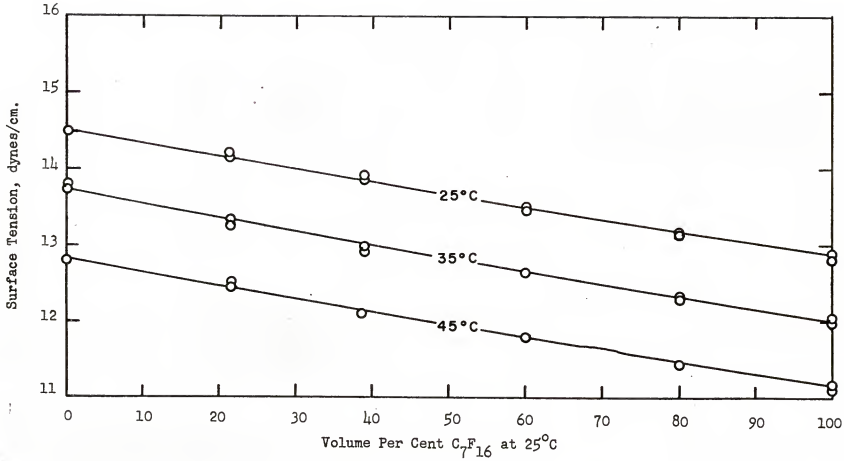

Figure 11.--Surface Tensions of the C_7F_{16} - $C_8F_{16}O$ System

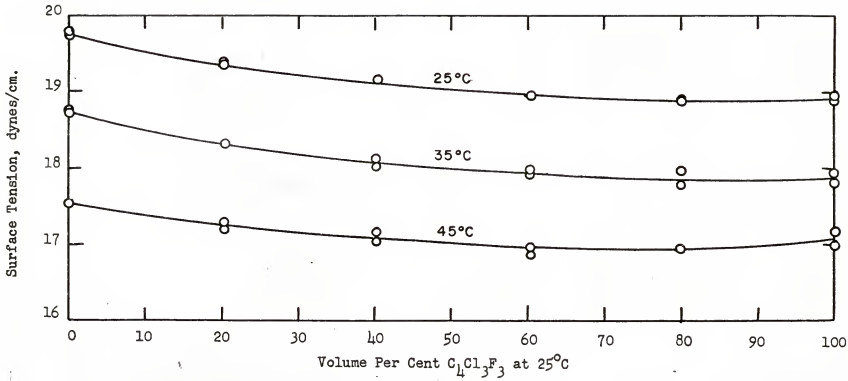

Figure 12.--Surface Tensions of the $C_5Cl_2F_6$ - $C_4Cl_3F_7$ System

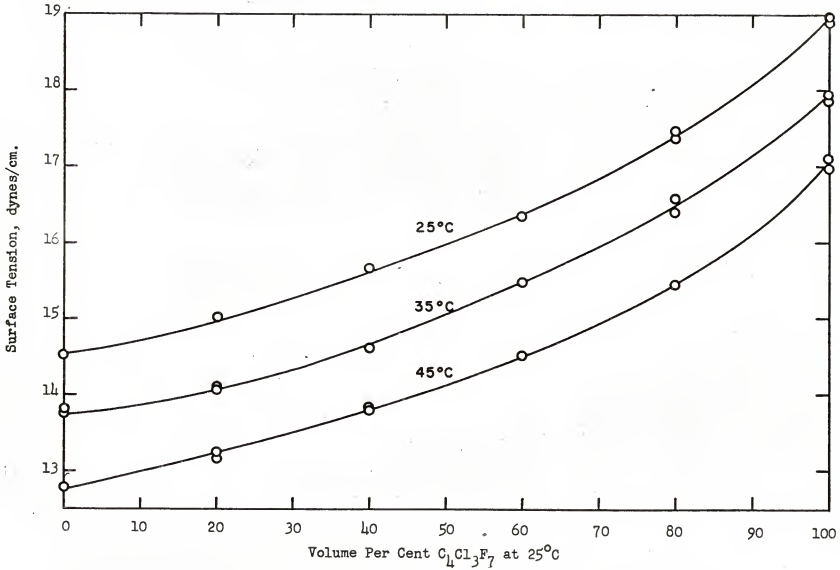

Figure 13.--Surface Tensions of the $C_4Cl_3F_7$ - $C_8F_{16}O$ System

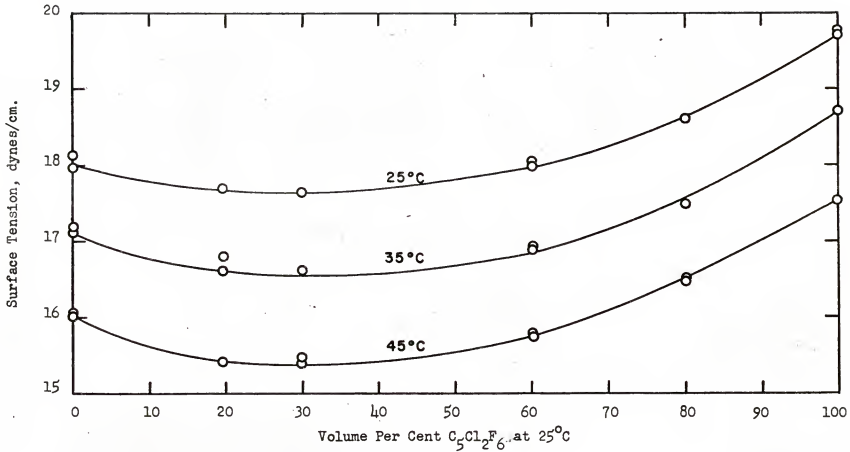

Figure 14.--Surface Tensions of the n-C_6H_{14} - $C_5Cl_2F_6$ System

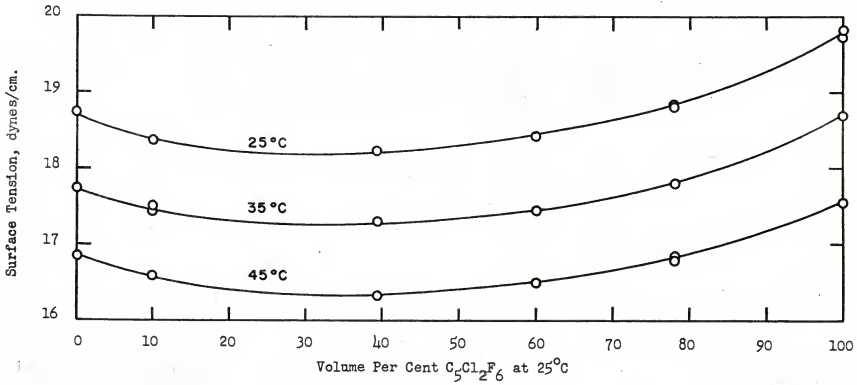

Figure 15.--Surface Tensions of the $C_5Cl_2F_6$ - i-C_8H_{18} System

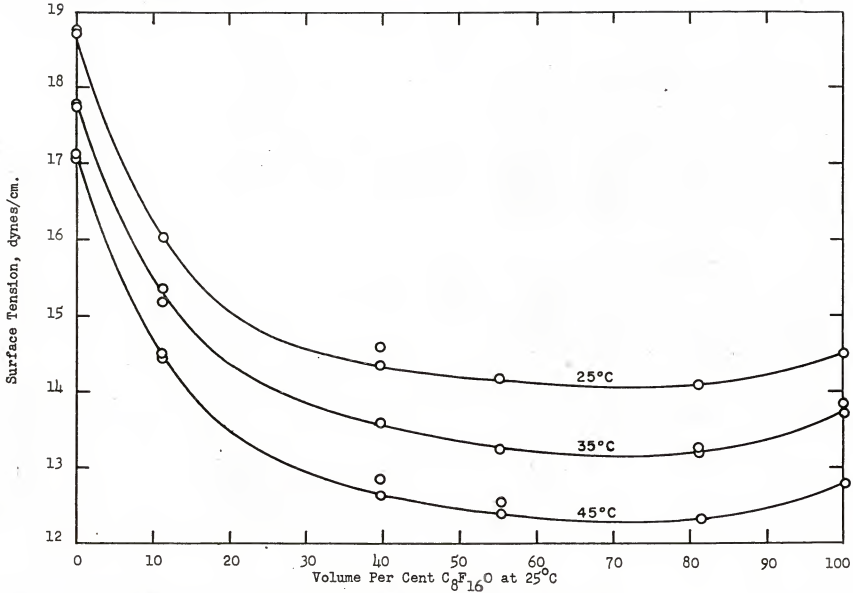

Figure 16.-- Surface Tensions of the 1-C_8H_{18} - $C_8F_{16}O$ System

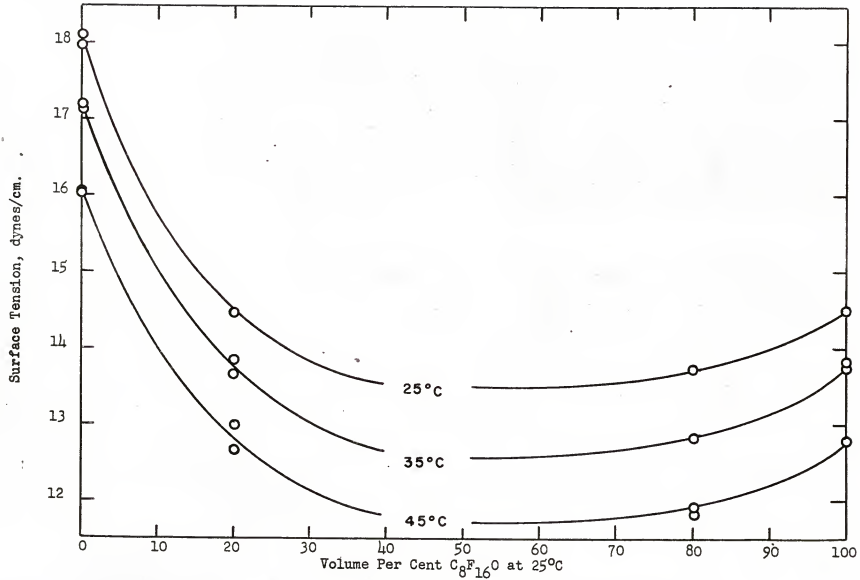

Figure 17.--Surface Tensions of the $\underline{n}$-C_6H_{14} - $C_8F_{16}O$ System

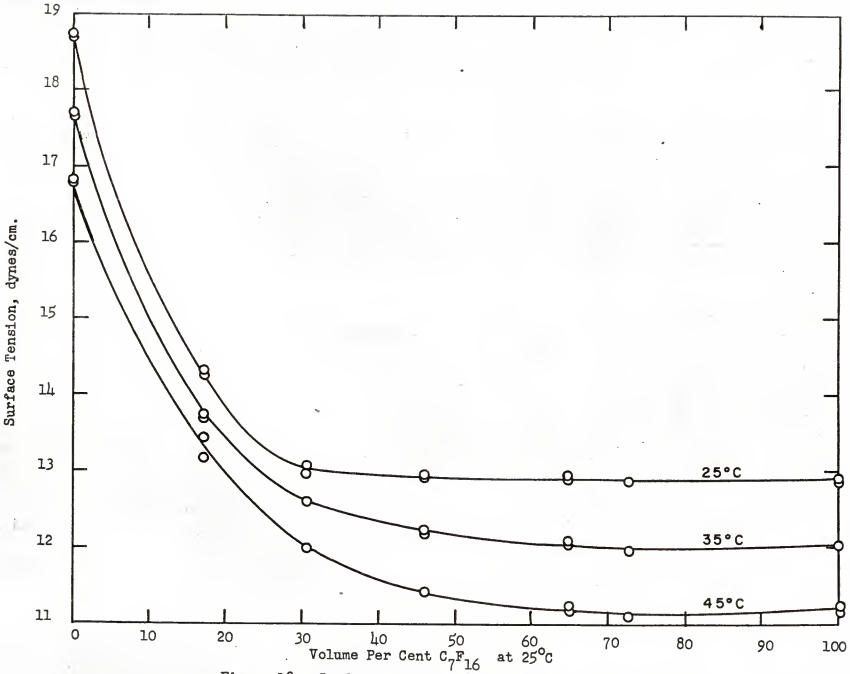

Figure 18.--Surface Tensions of the i-C_8H_{18} - C_7F_{16} System

Relative Surface Tensions by a Differential Capillary Rise Method. Due to the lack of both precision and accuracy encountered in the drop-weight surface tension determinations, a new apparatus has been designed which will permit the measurement of relative surface tensions with a high degree of accuracy.

The major problem in the drop-weight method is that the size of the drop is dependent upon its rate of formation. Similar problems are present in any procedure in which the surface area is varying at the time of measurement. While the capillary rise method is free from this objection, several other difficulties are encountered. In the apparatus designed in this work three of the major sources of error are eliminated.

Jones and Ray [51] have developed an equation for surface tensions using the capillary rise method:

$$\frac{\sigma_c}{\sigma_o} = \frac{(D_c-\beta_c)}{(D_o-\beta_o)}\left[1 + \frac{1}{\pi R^2 h_o(1-r/R)}\left(\frac{W_o}{D_o} - \frac{W_c}{D_c}\right)\right]$$

where:

σ = surface tension

D = density of liquid

β = density of gas phase (air and vapor)

W = weight

R = radius of large tube

r = radius of capillary tube

h = true capillary rise above infinite surface

subscripts:

o = reference liquid

c = test liquid.

The above equation does not assume:

1. Infinite reservoir
2. Any particular shape of meniscus
3. Uniform capillary
4. Optically uniform apparatus.

Jones and Ray measured h_o, r and R independently. This can, however, be avoided by writing the equation as

$$\frac{1}{\pi R^2 h_o(1-r/R)} = \text{constant (at each T)} = \left[\frac{\sigma_c(D_o-\beta_o)}{\sigma_o(D_c-\beta_c)} - 1\right] \Big/ \left(\frac{W_o-W_c}{D_o\ D_c}\right).$$

This constant may be evaluated if two standards are available (substitute for σ_c and σ_o in the last equation).

In practice enough material is added to the large tube to bring the liquid level in the capillary exactly to an etched mark. This amount of material is determined by the weight.

D_o, β_o and W_o are constants which must be evaluated at each T.

σ_o is a known constant or $\frac{\sigma_c}{\sigma_o}$ may be used to give the relative surface tensions.

D_c, β_c and W_c must be determined for each surface tension experiment.

R must be of uniform inside bore over the working range. Such tubes of extremely uniform bore are commercially available.

The liquid height in the capillary must be observed from the same height and angle so that any optical distortions are compensating and the apparatus must be aligned in the bath in the same manner for each determination. A permanently mounted support can assure this alignment.

Liquid Rise on Glass Walls. One of the most unusual properties of the systems studied is that certain of the mixtures will "creep" as a thin film up the glass walls of the apparatus in a manner highly suggestive of the well-known super-fluidity of liquid helium.

Of the binary mixtures studied, systems seven ($C_5Cl_2F_6$ - i-C_8H_{18}), eight (i-C_8H_{18} - $C_8F_{16}O$), and ten (C_7F_{16} - i-C_8H_{18}) exhibited this unusual behavior. This phenomenon was observed in the hydrocarbon-rich mixtures of these systems. Isooctane is the only material common to all three of these systems, and as a pure material, it does not creep up glass walls.

The most pronounced case was that of the C_7F_{16} - i-C_8H_{18} mixture containing 12.13 volume per cent fluorocarbon. For this mixture at room temperature the liquid rose to a level approximately 8 cm. above the meniscus of the bulk of the liquid. Creeping was observed to a lesser degree for mixtures containing up to 40 per cent C_7F_{16}, above which composition the phenomenon did not occur.

For system eight, a vertical creep of 2.5 cm. was observed at room temperature for the 11.18 volume per cent $C_8F_{16}O$ mixture although none was observed in the mixtures composed predominantly of fluorocarbon. System seven showed this phenomenon to a lesser degree in the mixtures containing less than 40 per cent of the chlorofluorocarbon.

The systems which creep up the glass walls all show minimums in the surface tension. An explanation based upon this fact alone is not adequate, however, as the $C_8F_{16}O$ - n-C_6H_{14} system (Figure 17) shows a much deeper minimum than the $C_5Cl_2F_6$ - i-C_8H_{18} system (Figure 15) and the former system does not exhibit this unusual behavior while the latter one does.

V. CALCULATIONS FROM VISCOSITIES OF BINARY SYSTEMS

Free Energy of Activation for Viscous Flow. Eyring et al. [32] have applied the theory of absolute reaction rates to the viscosities of liquids. According to this model, flow is pictured as a molecule reaching an activated state as it squeezes past its neighbors and then dropping into the next available equilibrium position. In this theory, the absolute viscosity is expressed as

$$\eta = \left(\frac{\lambda}{a}\right)^2 \frac{hN}{V} e^{\Delta G^*/RT} \tag{1}$$

where:

λ = distance between adjacent moving layers of molecules,

a = distance through which the shearing force acts,

h = Planck's constant,

N = Avogadro's number,

V = molar volume,

ΔG^* = free energy of activation,

R = gas constant, and

T = absolute temperature.

For ideal solutions in the thermodynamic sense it has been suggested [32, 36] that the viscosity be given by

$$\ln \eta_s = X_a \ln \eta_a + X_b \ln \eta_b. \tag{2}$$

Since the volume of a solution varies with the composition, it seems more reasonable to replace equation 2 by

$$\ln \eta_s V_s = X_a \ln \eta_a V_a + X_b \ln \eta_b V_b. \tag{3}$$

If equation 3 is used as the definition of ideal solution behavior in the viscosity sense and (λ/a) is set equal to unity, the free energy of activation for an ideal solution is linear in mole fraction, i.e.,

$$\Delta G_s^{*i} = X_a \Delta G_a^* + X_b \Delta G_b^*. \tag{4}$$

For non-ideal solutions, the observed free energy of activation will differ from the ideal value by a term g(x) which is a function of concentration:

$$\Delta G_s^* - \Delta G_s^{*i} = g(x). \tag{5}$$

By assuming (λ/a) is unity ΔG_s^*, values have been calculated by equation 1 and the points in Figures 1 through 10. The ΔG^* values calculated in the same way for the pure components were used in equation 4 to give the ideal solution values ΔG_s^{*i}. The difference between these values, g(x), is plotted for the 25°C and 45°C isotherms for systems one through ten in Figures 19 through 28, respectively.

It should be recalled that systems one through ten represent a steady departure from ideality in the thermodynamic sense. The viscosity of system one is essentially ideal and g(x) has very small positive values (Figure 19) corresponding to the small negative volume changes on mixing. System two, which is also ideal thermodynamically, is far from ideal in viscosities. Figure 20 shows that g(x) has rather

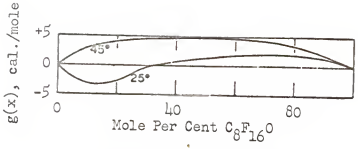

Figure 19.--Excess Free Energies of Activation for the C_7F_{16} - $C_8F_{16}O$ System

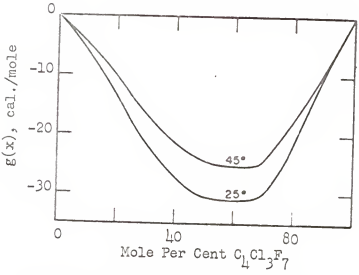

Figure 20.--Excess Free Energies of Activation for the $C_5Cl_2F_6$ - $C_4Cl_3F_7$ System

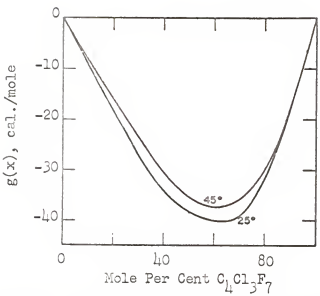

Figure 21.--Excess Free Energies of Activation for the $C_4Cl_3F_7$ - $C_8F_{16}O$ System

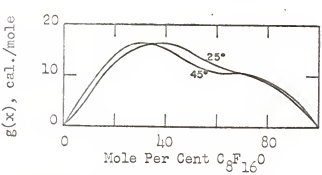

Figure 22.--Excess Free Energies of Activation for the $C_5Cl_2F_6$ - $C_8F_{16}O$ System

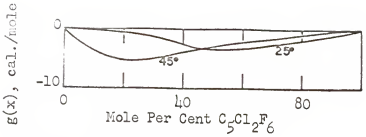

Figure 23.--Excess Free Energies of Activation for the $C_5Cl_2F_6$ - C_7F_{16} System

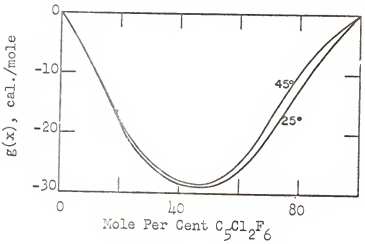

Figure 24.--Excess Free Energies of Activation for the n-C_6H_{14} - $C_5Cl_2F_6$ System

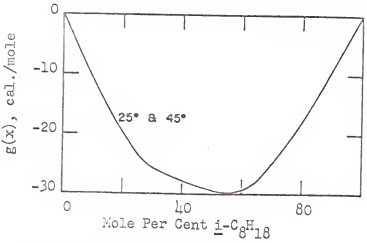

Figure 25.--Excess Free Energies of Activation for the $C_5Cl_2F_6$ - i-C_8H_{18} System

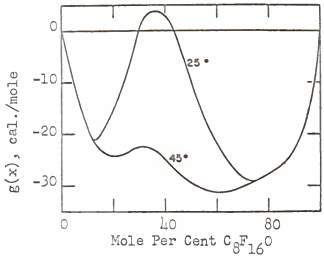

Figure 26.--Excess Free Energies of Activation for the i-C_8H_{18} - $C_8F_{16}O$ System

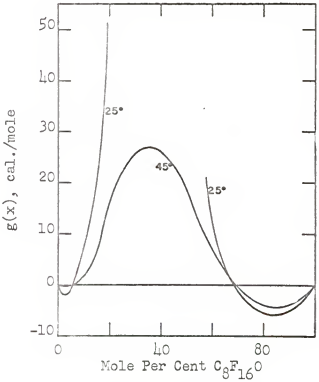

Figure 27.--Excess Free Energies of Activation for the n-C_6H_{14} - $C_8F_{16}O$ System

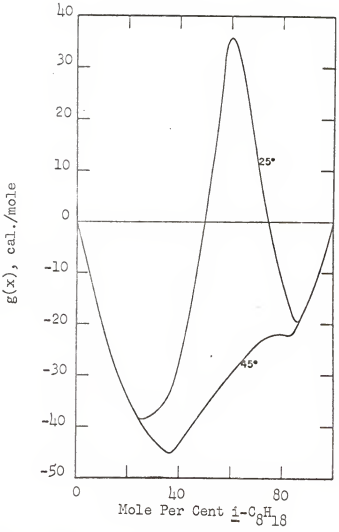

Figure 28.--Excess Free Energies of Activation for the $\underline{i}$-C_8H_{18} - C_7F_{16} System

large negative values over the whole composition range. System five, on the other hand, is not ideal thermodynamically but g(x) has relatively small negative values (Figure 23). The fourth combination is illustrated by system three, which is far from ideal both in its viscosity behavior (Figure 21) and in its thermodynamic behavior.

System four (Figure 22) is particularly interesting in that it displays large positive values for g(x) when all the other systems from two through seven have negative values for g(x). Each one of these six systems shows expansion on mixing.

It is immediately apparent that there is no simple correlation between non-ideal behavior in the thermodynamic sense and non-ideal behavior in the viscosities of solutions. At least two general effects may be singled out from these studies. The more obvious one is illustrated by systems six and seven (Figures 24 and 25), where expansions on mixing are accompanied by decreases in the free energy of activation for viscous flow.

To account for the decrease in ΔG_s^* due to expansion on mixing, g(x)/RT has been plotted versus the total volume change on mixing in Figure 29 for systems six, seven, and ten. For the first two of these systems, Figures 29A and 29B, the lowering of viscosities of the solutions may be attributed directly and entirely to the expansion on mixing.

From the 25°C isotherm of Figure 29C, it is obvious that a second effect in the viscosities exists. This effect corresponds to the inflections in g(x) for systems eight, nine, and ten, Figures 26 through 28, respectively. In these three figures the curves near the edges of the

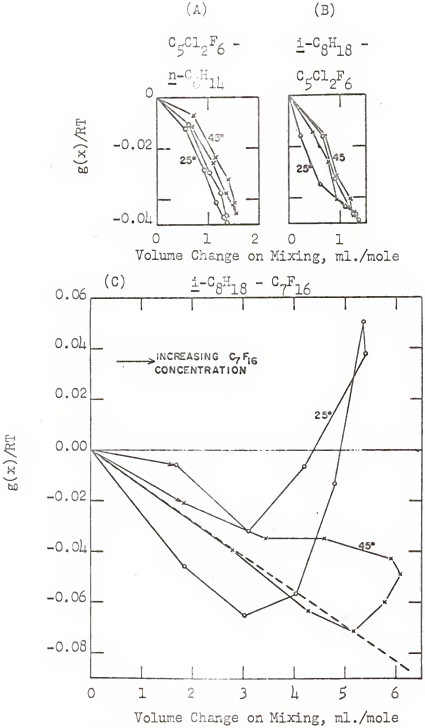

Figure 29.--Excess Free Energy as a Function of Volume Change on Mixing

figures, i.e., the dilute solutions, resemble Figures 24 and 25 in which the viscosity lowering is attributed to the volume change on mixing. Near the center of Figures 24 through 28, a second effect is obviously superimposed on the expansion effect.

This second effect will be interpreted in terms of an association or local clustering within the solution. This effect is noticeable for system ten at 45°C, some 21C° above the maximum unmixing temperature. At lower temperatures this effect predominates over the expansion on mixing effect and the ΔG_s^* becomes greater than the ideal ΔG_s^{*i}. From Tables 10 through 12, it can be seen that the volume changes on mixing show no inflections corresponding to these increasing values of g(x). Similarly, Figure 29C shows that both the expansion effect (dashed line), and the clustering effect (pronounced rise in g(x) at 25°C) are present.

The positive g(x) values observed over the entire composition range for system four, Figure 22, suggest that the second effect is overwhelmingly large compared to the expansion on mixing effect. The fact that g(x) in system five has such small negative values, out of proportion to the expansion, no doubt arises from the interplay of both effects in this solution. Systems four and five are similar to systems one, two, three, six, and seven in that the thermodynamic free energies of mixing are not sufficiently large to produce partial miscibility. Inasmuch as they show a dominating value for the second effect, these solutions are similar to those solutions (eight, nine, and ten) which have large thermodynamic free energies of mixing. The conclusion to be drawn from these similarities and differences is that the second effect

is associated with the thermodynamic entropy of mixing for the solutions. We will see that the positive part of g(x) may be accounted for by allowing λ/a to be a variable in equation 1.

The Factor λ/a as a Variable. By differentiating ln ηV in equation 1 with respect to 1/T at constant composition one obtains

$$\frac{\partial \ln(\eta V)}{\partial(1/T)} = \frac{1}{R}\,\frac{\partial(\Delta G^*/T)}{\partial(1/T)} + 2\,\frac{\partial \ln(\lambda/a)}{\partial(1/T)}. \tag{6}$$

Rearranging gives an expression for the enthalpy of activation ΔH^*,

$$\frac{\partial(\Delta G^*/T)}{\partial(1/T)} = \Delta H^* = R\,\frac{\partial \ln(\eta V)}{\partial(1/T)} - 2R\,\frac{\partial \ln(\lambda/a)}{\partial(1/T)}. \tag{7}$$

From the experimental viscosities, it was found that ln ηV versus 1/T gave essentially a straight line over the temperature range studied. This was true for the pure materials and for the mixtures which showed no inflection point in g(x). Thus, for these cases, at each composition the quantity $\partial \ln \eta V/\partial(1/T)$ is a constant independent of temperature. In systems eight, nine, and ten, however, where g(x) shows maxima and minima with respect to change in composition, $\partial \ln \eta V/\partial(1/T)$ varies with temperature in a manner illustrated by Figure 30 for some data of system ten. The maximum unmixing temperature of 23.65°C for this system occurs at 61.4 mole per cent isooctane (54 volume per cent at 25°C). As the temperature for this composition is lowered, $\partial \ln \eta V/\partial(1/T)$ shows a rapid rise beginning in the neighborhood of 27°C. At 27°C, $R\partial \ln \eta V/\partial(1/T)$ is 4000 calories per mole and rises to 87,000 calories per mole at 23.7°C. In the dilute solutions, even for these systems (eight, nine, and ten), $\partial \ln \eta V/\partial(1/T)$ is a constant independent of temperature.

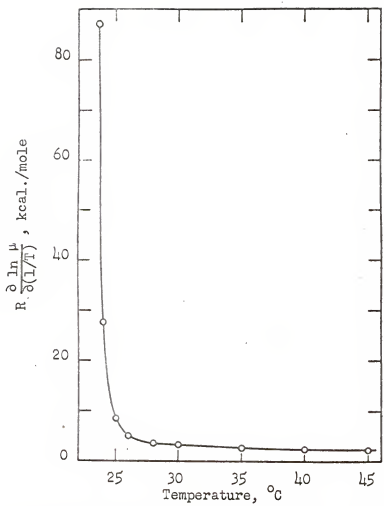

Figure 30.--R ∂ ln μ/∂(1/T) as a Function of Temperature for the i-C_8H_{18} - C_7F_{16} System

As an hypothesis to explain these observations, we will assume the following schemes for the flow process.

I. In pure liquids or in solutions where no exaltation of g(x) is observed,

$$A_1 \rightarrow A^* + \text{hole} \rightarrow A_2 \qquad \text{(I)}$$

II. In liquids where g(x) shows the exaltation,

$$A_1^n \rightarrow nA^* + n \text{ holes} \rightarrow A_2^n \qquad \text{(II)}$$

In I, A_1 represents a molecule in position 1, A^* represents the molecule in the activated state, and A_2 is the molecule displaced to position 2. In II, A_1^n represents n molecules in some group or association (e.g., in the incipient two-phase region at temperatures just above the unmixing temperature). A_2^n represents the molecules displaced to new positions and included in a new group.

The enthalpies of activation per mole, ΔH^*, in a given liquid for process I and for process II are essentially identical, since the holes required possess the same properties in both processes. Thus, ΔH^* will be a function only of composition in either process I or II. In the temperature region where the viscosity or g(x) versus composition show the maxima, under these hypotheses, the excessively high temperature coefficient of viscosity, and of g(x) above those values expected in the absence of the grouping effect, must be exactly compensated by the term $-2R\ \partial \ln(\lambda/a)/\partial(1/T)$ in equation 7. It is shown in the following paragraphs that this is true. This hypothesis thus attributes a positive portion of the total g(x) to a change in cluster size with

temperature. The shearing force acts on an area λ^2 which is larger when clusters are present than when they are absent.

Classification of Viscosity of Solutions. A more explicit form of equation 5 is needed which includes values of λ/a different from unity. From equation 1 we may write for the solution

$$\ln(\eta_s V_s/hN) = \Delta G_s^*/RT + \ln(\frac{\lambda}{a})^2. \tag{8}$$

If we then write,

$$\ln(\eta_s V_s/hN) = x_a[\Delta G_a^{*o}/RT + \ln(\lambda/a)_a^2] + x_b[\Delta G_b^{*o}/RT + \ln(\lambda/a)_b^2]$$
$$+ g_v(x)/RT + \ln f \tag{9}$$

the term ln f is defined by,

$$\ln f = \ln(\lambda/a)_s^2 - x_a\ln(\lambda/a)_a^2 - x_b\ln(\lambda/a)_b^2. \tag{10}$$

Then the g(x) of equation 5 becomes

$$g(x) = g_v(x) + RT \ln f, \tag{11}$$

in which $g_v(x)$ is that part of g(x) which arises from the change in volume on mixing. Equations 7, 9, 10, and 11 serve as the basis for classifying the viscosity behavior of solutions:

1. For ideal solutions both $g_v(x)$ and ln f are zero. Thus g(x) is zero and the ideal solution obeys equation 3. The two fluorocarbons, C_7F_{16} and $C_8F_{16}O$, which constitute system one, are very close to this behavior.

2. For this class of solution g(x) is not zero but $[\partial\ln(\eta V)/\partial(1/T)]_x$ is independent of temperature and (λ/a) is independent

of temperature for any given composition. Subclasses would be those for which $g(x)$ is positive or for which $g(x)$ is negative.

3. The third type of mixture is that in which $[\partial \ln(\eta V)/\partial(1/T)]_x$ is a function of temperature. Systems eight, nine, and ten fall in this class.

Treatment of Class 3 Solutions. At sufficiently high temperatures Class 3 solutions behave like Class 2 solutions and for each composition ΔH^* is a constant by equation 7 since $[\partial \ln(\lambda/a)/\partial(1/T)]_x$ is then equal to zero. These values of ΔH_s^* agreed within a few per cent of those calculated by assuming ΔH_s^* was ideal, i.e.,

$$\Delta H_s^{*i} = X_a \, \Delta H_a^* + X_b \, \Delta H_b^* \tag{12}$$

These ideal values of ΔH_s^{*i} were used in these calculations. Using these values in equation 7, $[2 \, \partial \ln(\lambda/a)_s/\partial(1/T)]_x$ may be evaluated. According to equation 10,

$$\left(\frac{\partial \ln f}{\partial \, 1/T}\right)_x = 2\left(\frac{\partial \ln(\lambda/a)_s}{\partial(1/T)}\right)_x \tag{13}$$

since $\partial \ln(\lambda/a)/\partial(1/T)$ is assumed to be zero for the pure compounds. This last is taken to be true since, as with Class 2 solutions, $\partial \ln(\eta V)/\partial(1/T)$ is independent of temperature for the pure components.

Substitution of equation 13 into equation 7 and integrating between T_1 and T_2 at a given composition gives,

$$\ln \frac{f_2}{f_1} = \ln \frac{(\eta V)_2}{(\eta V)_1} - \frac{\Delta H^*}{R}\left[\frac{1}{T_2} - \frac{1}{T_1}\right]. \tag{14}$$

Since the composition is fixed

$$\frac{(\eta V)_2}{(\eta V)_1} = \frac{(\eta/\rho)_2}{(\eta/\rho)_1} = \frac{\mu_2}{\mu_1} \tag{15}$$

where μ is the kinematic viscosity. Using kinematic viscosities in equation 14 and the ideal ΔH_s^* values discussed above gives the ratio of shape factors $\frac{f_2}{f_1}$ at two temperatures.

The difference in $g(x)/RT$ for the two temperatures is given by equation 11 as

$$g(x)_2/RT_2 - g(x)_1/RT_1 = g_v(x)_2/RT_2 - g_v(x)_1 RT_1 + \ln f_2/f_1. \tag{16}$$

It is shown in Figures 29A and 29B that $g_v(x)/RT$ at two temperatures, 25°C and 45°C, are essentially equal if the volume change on mixing is not very different at the two temperatures. Setting $g_v(x)_1/RT_1 = g_v(x)_2/RT_2$ and combining equations 11, 14, and 15 gives

$$g(x)_1/RT_1 = g(x)_2/RT_2 - \ln \mu_2/\mu_1 + (\Delta H^*/R)[1/T_2 - 1/T_1]. \tag{17}$$

Referring now to Figure 31 for system ten and taking $T_1 = 45°C$ and T_2 equal to the various temperatures between 45°C and the critical unmixing temperature, $g(x)/RT$ at 45°C has been computed from $g(x)/RT$ at lower temperatures by means of equation 17. The points shown on the figure are the values so computed. It is obvious that the theory accounts very well for the difference in $g(x)/RT$ between the lower temperatures and 45°C since the calculated points coincide almost exactly with the experimental curve at 45°C obtained from the viscosities alone at 45°C. The dashed curve drawn on Figure 31 is $g_v(x)/RT$ at 45°C estimated from the volume changes on mixing at each composition by means

of the dashed line drawn on Figure 29C. The same computation has also been made for the 25°C-curve of system eight (Figure 32). The points calculated from the data at 25°C fall on the curve for 45°C.

This agreement establishes the idea that the exaltation in the viscosity of these mixtures arises from a variation in $(\lambda/a)_s$ with temperature and with composition. The small magnitude of this variation is illustrated by values in Table 13. An increase of only about 6 per cent is sufficient to account for the greatest increase in viscosity at 25°C above the value expected from the volume change effect.

A value for the viscosity at the critical unmixing point ($T = 23.65°C$, $X = 0.614$ isooctane) for system ten has been estimated by extrapolating the value shown in Table 14 of $\ln f_T/f_{45}°$ at this composition. The kinematic viscosity at the critical point is 0.645 centistokes. λ/a at 23.65°C and 0.614 mole fraction isooctane is 15 per cent larger than its value at 45°C. From the dashed curve on Figure 31 a value for f/f_o at 45°C may be estimated as 1.04 at 0.614 mole fraction isooctane, so that f/f_o at the critical unmixing point is approximately 1.19.

Vapor-liquid equilibria of $\underline{n}$-C_7F_{16} with isooctane have been reported [69] at the three temperatures, 30°, 50°, and 70°C. The total excess free energy and entropy of mixing at these temperatures are positive. At the lower temperatures the excess entropy as a function of composition resembles the negative of the curve for $g(x)$ at 45°C on Figure 28. The increase in λ/a with decrease in temperature is accompanied by an increase in order among the molecules in the solution.

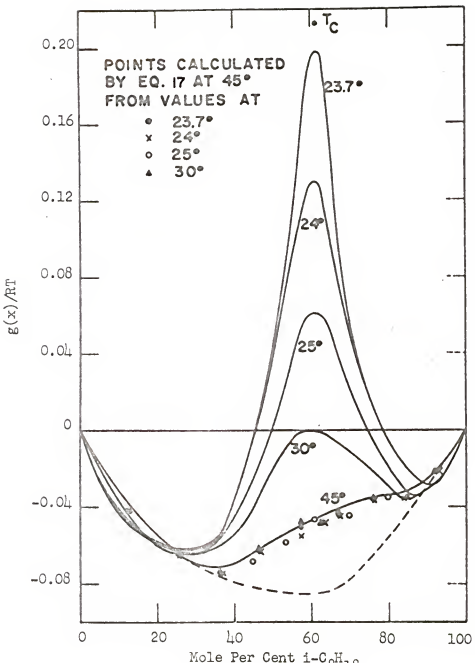

Figure 31.--Excess Free Energy Function for the i-C_8H_{18} - C_7F_{16} System

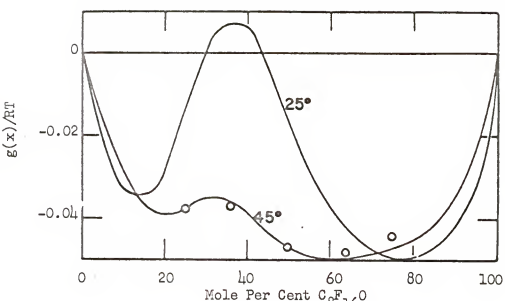

Figure 32.--Excess Free Energy Function for the i-C_8H_{18} - $C_8F_{16}O$ System

TABLE 13

Shape Factors for the i-C_8H_{18} - $C_8F_{16}O$ and i-C_8H_{18} - C_7F_{16} Systems

Mole Fraction	$2 \ln[f_{25}/f_{45}]$	f_{25}/f_{45}
	System 8: $C_8F_{16}O$ with i-C_8H_{18}	
$C_8F_{16}O$		
25	+0.0252	1.013
36	+0.0444	1.022
50	+0.0306	1.015
64	+0.0057	1.003
75	-0.0051	0.99
	System 10: i-C_8H_{18} with C_7F_{16}	
i-C_8H_{18}		
45	+0.0416	1.021
53.1	0.0790	1.040
61	0.1066	1.055
70	0.0660	1.034
80	0.0137	1.007

TABLE 14

Shape Factors at the Critical Composition for the $\underline{i}$-C_8H_{18} - C_7F_{16} System

T, °C	$2 \ln[f_T/f_{45°}]$	$f_T/f_{45°}$
	System 10 at the Critical Composition, 61.4 Mole Per Cent Isooctane	
23.65	(+0.2614)	1.15
23.7	0.2459	1.130
24	0.1777	1.093
25	0.1066	1.055
30	0.0461	1.023
45	0.0	1.00

This conclusion is also obvious from the behavior of the heat capacity of this solution in the neighborhood of the critical unmixing temperature [52].

Data [37] for methanol-toluene solutions fall into this class and fit equation 17. The maximum value for f_{25}/f_{45} for this system is 1.03 and occurs at approximately 75 mole per cent methanol.

Treatment of Class 2 Solutions. These mixtures are those for which the second viscosity effect (clustering) is not a function of temperature. Systems two, three, six, and seven fall in the subclass for which g(x) is negative for a positive volume change on mixing. Systems eight through ten would also fall into this subclass at sufficiently high temperatures or in the dilute solution regions. The subclass, for which g(x) is greater than would be expected from the expansion on mixing, is represented by systems four and five. Both positive and small negative g(x) value may occur in the latter subclass.

In mixtures such as system seven, for which g(x) is not a function of temperature (Figure 25)

$$\left(\frac{\partial g(x)}{\partial T}\right)_x = 0 \tag{18}$$

and from equation 11

$$\left(\frac{\partial g_v(x)}{\partial T}\right)_x = - R \ln f = - s_v(x). \tag{19}$$

Substitution in equation 11 then gives

$$g(x) = g_v(x) + T\ s_v(x) = h_v(x) \tag{20}$$

so that even though ln f is not necessarily zero, g(x) may depend upon the volume change for such systems.

System four has small positive volume changes accompanying mixing. Nevertheless, g(x) for this system is positive at all compositions (Figure 22). The positive portion of g(x) is far greater than the negative value of $g_v(x)$ in this system. If it be true in this case, as was suggested above for system ten, that large values of λ/a (and consequently large values of f by equation 10) mean abnormally low entropies of mixing, it should be expected that system four would exhibit negative excess entropies of mixing. The thermodynamics of mixtures of $C_8F_{16}O$ with $C_5Cl_2F_6$ should be interesting in this respect.

It has been postulated throughout that the enthalpy of activation is the same for a given mixture whether the process be I or II. By equation 7 this hypothesis leads to

$$[\partial \ln(\lambda/a)_s/\partial(1/T)]_x = C_x \tag{21}$$

as a characteristic of Class 2 solutions. C_x is a constant independent of temperature but a function of composition. In the treatment of Classes 2 and 3 we have taken C_x arbitrarily as zero, whenever $[\partial \ln \bar{V}/\partial(1/T)]_x$ is independent of T. If C_x is not zero, then the base ΔH^* appearing in equation (14) is actually $\Delta H^* + 2\,RC_x$. The treatment of Class 3 on this basis would not be altered.

VI. EXAMINATION OF THEORIES OF LIQUID VISCOSITY

In examining the various theories of viscosity, use has been made of 52 molecules. These molecules are listed in Table 15 together with the major sources of experimental data used.

Temperature Dependence of Viscosity. Of the numerous equations that have been advanced to describe the viscosity behavior of liquids, the one originally proposed by Reynolds [81] in 1886,

$$\eta = a\, e^{b/T} \tag{22}$$

is the most frequently used. Eyring *et al.* [32] have attempted to interpret the parameters a and b in terms of the "absolute reaction rate" theory of kinetics. The Eyring theory has been popular simply because it gives a fairly good empirical fit to the experimental data. The agreement, however, is far short of the precision available in viscosity measurements. When $\ln \eta$ versus $\frac{1}{T}$ is plotted over a wide temperature range, curves are obtained for practically all liquids. These curves have increasing slopes as the temperature decreases. In one of the attempts to obtain better agreement with experiment, Jobling and Lawrence [49, 50] have taken a more exact form of Eyring's theory which contains the volume dependence as well as that of Andrade [2] and proposed that $\ln \eta$ versus $\frac{1}{T}$ is linear only at constant volume. This frequently used idea [22, 65], known as the free volume approach, results in two difficulties. The first difficulty is that this approach

TABLE 15

Sources of Data for 52 Liquids Used to Test Viscosity Theories

Molecule	Viscosity references	Density references
Simple Molecules		
Ar	12, 8, 62, 60, 58, 56	82, 23, 21
Kr	12	21, 61
Xe	56	21
Hg	45, 53, 71	72, 46
N_2	8, 62, 60	
O_2	12, 62, 8	
F_2	78	78
CO	62	
CS_2	26, 46	29, 25
$CHCl_3$	25, 70	92, 29, 70
CCl_4	26, 46, 62, 25, 47, 70, 33	29, 25, 70, 33, 96
CBr_4	30	30
Paraffins		
CH_4	1, 12, 8, 16, 86, 62	23, 1
C_2H_6	1, 86,	1
C_3H_8	1, 86, 85	1
n-C_4H_{10}	1, 86	1
i-C_4H_{10}	1	1

TABLE 15 (Continued)

Molecule	Viscosity references	Density references
Paraffins (Continued)		
n-C_5H_{12}	1, 47	1, 55
i-C_5H_{12}	1,	1, 46, 55
neo-C_5H_{12}	1, 89, 73	1
n-C_6H_{14}	1, 47	1, 55
n-C_7H_{16}	1	1
n-C_8H_{18}	1	1
2 Me heptane	31	31
3 Me heptane	31	31
4 Me heptane	31	31
3 Et hexane	31	31
2,2 di Me hexane	31	31
3,3 di Me hexane	31	31
2,4 di Me hexane	31	31
2,5 di Me hexane	31	31
3 Me,3Et pentane	31	31
2,2,3 tri Me pentane	31	31
2,3,3 tri Me pentane	31	31
2,3,4 tri Me pentane	31	31
n-C_9H_{20}	1	1
n-$C_{10}H_{22}$	1, 70	1, 70

TABLE 15 (Continued)

Molecule	Viscosity references	Density references
Cyclo paraffins		
cy-C_5H_{10}	1	1
cy-C_6H_{12}	33, 47	95, 33, 27
Me cyclohexane	1	27
Aromatics		
benzene	1, 38, 62, 60, 47, 33	33, 1
toluene	1	1, 29
Fluorocarbons		
n-C_5F_{12}	78	78
n-C_6F_{14}	78	78
n-C_7F_{16}	80	80, 84
cyclo-C_5F_{10}	78	
Other Molecules		
H_2O	45, 53, 46	46
Methanol	46	29
Ethanol	92	29
acetone	46	29, 46
di Ethylether	25, 46	25
chloro benzene	25	25

is based upon the equation for viscosity,

$$\eta V^{1/3} = a\ e^{c/VT} \tag{23}$$

in which V is the molar volume. That this is not the correct relationship is easily verified by plotting $\ln (\eta/\rho^{1/3})$ versus ρ/T which gives curves similar to those for $\ln \eta$ versus $1/T$ described above. The second difficulty is that for at least one liquid (CO_2) this approach, with the data of Jaeger [48], gives negative values for the activation energy for flow.

Following a similar line of reasoning, Doolittle and Doolittle [24] have suggested

$$\ln \eta = a + \frac{b\ V_o}{(V-V_o)} \tag{24}$$

where V_o is the volume of the liquid extrapolated to 0^oK. This equation, in terms of statistical treatments of the hole theory by Weymann [94] and Cohen and Turnbull [18], was incorporated by Macedo and Litovitz [59] into a "hybrid equation,"

$$\eta = a_o\ e^{bV_o/(V-V_o)}\ e^{\Delta E^*_{vis}/RT} \tag{25}$$

where the last term is taken from Eyring's form of equation 22,

$$\eta = a\ e^{\Delta E^*_{vis}/RT}. \tag{26}$$

While neither equation 24 nor equation 26 with constant parameters give good correlations over extended temperature ranges, equation 25 is some improvement since it contains an additional adjustable parameter.

Following Macedo and Litovitz, b is set equal to unity in equation 25, V is replaced by A and B values [78] from

$$V^{-2} = A - BT \tag{27}$$

(an equation satisfied within approximately 0.1 per cent in density in these temperature ranges by all of the liquids used), and equation 25 becomes

$$\ln \eta = \ln a_o + \{[1 - (B/A)T]^{-1/2} - 1\}^{-1} + \Delta E^*_{vis}/RT \ . \tag{28}$$

Plots of $[\ln \eta + \{1 - (1 - T\frac{B}{A})^{-1/2}\}^{-1}]$ versus 1/T imply negative activation energies which vary with temperature for 19 of the 25 compounds tested. If, following Weymann's argument [94], a_o is considered to be temperature dependent and given by

$$a_o = \left(\frac{RT}{\Delta E^*_{vis}}\right)^{1/2} \frac{(2\ mkT)^{1/2}}{V^{2/3}} \ , \tag{29}$$

two values of ΔE^*_{vis} may be obtained. One is obtained from the intercept and the other from the slope of $\left[\ln (\eta \frac{V^{2/3}}{T}) - \frac{V_o}{(V-V_o)}\right]$ versus 1/T. The two values obtained for n-hexane were +2.7 kcal./mole and -9.6 kcal./mole, respectively. Writing $a_o = a'T$ also gave negative ΔE^*_{vis} values by equation 25. As a final alternative to maintain the fit achieved by equation 25, ΔE^*_{vis} is interpreted by the authors according to equation 26 for some compounds as

$$\Delta E^*_{vis} = \left(\frac{\partial \ln \eta}{\partial (1/T)}\right)_p \tag{30}$$

and, in other cases as

$$\Delta E^{*}_{vis} = \left(\frac{\partial \ln \eta}{\partial(1/T)}\right)_{v} . \tag{31}$$

These values, however, can differ by a factor of five [26, 49].

Various equations have been suggested by many authors (e.g., [32, 45, 53, 60, 87, 88, 90, 91]), which may be included under the general forms

$$\ln \eta \rho^{n} = a + \frac{b}{T} \tag{32}$$

or

$$\ln \eta T^{m} = a + \frac{b}{T} \tag{33}$$

in which n and m have values which vary widely from one author to another. Since particular ones of these equations provide better fits than do others for various compounds, no general correlation will be found in these forms and they should be viewed as empirical. Best fits of the experimental data by equations 32 and 33 were found in this work to require widely varying values of n or m even within the homologous series of normal alkanes.

In the present work it was observed that $\partial \ln \mu/\partial(1/T)$ varied more widely with temperature than did $\partial \ln \eta/\partial(1/T)$. Since $\mu = \eta/\rho$, this suggested plotting $\ln \eta\rho$ versus $1/T$. This strictly empirical plot provides a marked improvement in linearity over that obtained from equation 26. This linearity was found to be true even for methanol for which Innes [45] reports that m = 0 in equation 33.

The point to be made here is that viscosity varies much more rapidly with temperature than does density so that over small temperature

intervals the effect of density variation is minor. Simple relations between these two quantities should be viewed as empirical and for data at atmospheric pressure or low pressures

$$\ln \eta_\rho = a + \frac{b}{T} \tag{34}$$

is a better two-constant empirical equation than any in current widespread use. Equation 34 applies over the whole liquid range for a particular compound.

Corresponding States for Pure Materials. Reed and McKinley [79] have shown that the A and B of equation 27,

$$V^{-2} = A - BT$$

which describes liquids at temperatures below $T = 0.8T_c$, may be related to E^*, r^*, m, and n of a Lennard-Jones bireciprocal pair-potential energy function,

$$E(r) = \frac{E^*}{(n-m)}\left[m\left(\frac{r^*}{r}\right)^n - n\left(\frac{r^*}{r}\right)^m\right], \tag{35}$$

where:

m = attraction exponent,

n = repulsion exponent,

E^* = depth of the pair-potential energy minimum, and

r^* = distance between molecular centers at E^*.

Since $A^{-1/2}$ equals the molar volume extrapolated to absolute zero,

$$(r^*)^3 = \gamma^* V_o = \gamma^*/A^{1/2} . \tag{36}$$

Also,

$$\left(\frac{A}{B}\right) = \frac{E^*}{kKY} \tag{37}$$

where k = Boltzmann's constant and γ^* and KY are constant for a given m and n. If the following conditions are fulfilled, it should be possible to use A and B to reduce the viscosities and obtain a universal function obeyed by all liquids:

1. The potential of interaction is the sum of pair interactions.
2. Pair interactions may be written in the same form (e.g., equation 35 with fixed values for m and n).
3. The partition function may be factored into translational, vibrational, rotational and internal parts, and the translational part is the only one that depends upon the volume per molecule.

This suggests that by means of dimensional analysis the reducing factors may be found for the various properties of the liquid. The reduced property obtained should then be a universal function of the reduced temperature. Such calculations have been quite successful in correlating thermodynamic and transport gas phase properties for these compounds [79, 6]. A and B values were calculated from liquid densities and are given in Table 16. Other values were taken from Reed et al. [79, 6, 17].

Absolute viscosity, η, has units of mass/(length x time) which means that the reducing factor is $[(m\,E^*)^{1/2}\,r^{*-2}]^{-1}$. Using A and B from equations 36 and 37, the reduced absolute viscosity, η_r, becomes

$$\eta_r = \eta\,\frac{(B/A)^{1/2}}{A^{1/3}\,M^{1/2}} \tag{38}$$

where M is the molecular weight. η_r plotted against a reduced temperature,

$$T_r = T\left(\frac{B}{A}\right) , \tag{39}$$

TABLE 16

Liquid Density Parameters A and B
from Equation 27

Molecule	A, 10^{-4}(mole/cc.)^2	B, $\frac{mole^2}{cc.^2\ {}^oK}$
CH_4	12.2598	47.2516
i-C_4H_{10}	2.0512	3.86182
n-$C_{10}H_{22}$	0.4221	0.5405
cyclo-C_5H_{10}	2.0173	3.02752
Toluene	1.4371	1.88001
Methanol	10.3584	14.5256
Ethanol	4.7866	6.31363
Diethylether	1.8081	3.00641
Acetone	3.4029	5.29369
$CHCl_3$	2.7154	3.95722
CS_2	4.6667	6.52388
CBr_4	1.23	1.16
Hg(0-70°C)	50.5116	16.6053

should give one curve if the above conditions are fulfilled. Actually, a series of curves was obtained. The normal alkanes formed a family of curves which were crossed by the more symmetrical hydrocarbon, CCl_4, and the fluorocarbon curves. Reduced kinematic viscosities,

$$\mu_r = \mu(\frac{EM}{A})^{1/2} A^{1/6} , \tag{40}$$

plotted against T_r from equation 39 gave an almost identical pattern of curves.

A number of other combinations were attempted but in each case essentially the same pattern of curves was obtained as resulted when η_r was plotted versus T_r. Some of these reduced properties plotted versus T_r were $[\eta/(\rho)^{1/2}]_r$ after Thomaes[89], $[\eta V]_r$, and $[\eta V^2]_r$. Collins and Raffel's [20] statistical treatment of transport leads to

$$\eta^2 = 0.510\ (\rho/V^{1/3})(-2.4E_{vap} - kT + pV). \tag{41}$$

Reduction by A and B gives

$$\eta^2/(TMA^{2/3}) = f(TB/A) \tag{42}$$

where f should be a universal function. $\eta^2/(TMA^{2/3})$ versus TB/A once again gave the pattern of curves discussed above. The dimensionless reduced viscosity of equation 42 is similar to that of equation 38 with E^* replaced by kT.

The molecules having curves crossing the majority of the other curves in the above treatments were those which have relatively short liquid ranges. Plots of η_r, μ_r, as well as η and μ, were made versus both $\frac{T - T_m}{T_b - T_m}$ and $\frac{T - T_c}{T_c - T_m}$ where the subscripts b, m, and c denote the

normal boiling point, normal melting point, and the critical temperature [1, 54, 7], respectively. The η_r versus $\frac{T - T_m}{T_c - T_m}$ plot gave the only set of parallel curves obtained for the molecules tested. Attempts to correlate the constants required to move these curves together with properties of the compounds were unsuccessful.

In most theories of viscosity the exponent factor b in equation 22 is considered to be proportional to an energy as shown in equation 26. This energy, ΔE^*_{vis}, was plotted versus the energy factor A/B in these reducing parameters. A single curve resulted for the normal paraffins and many other organic compounds (Figure 34). The most notable departures from this curve are those molecules with the exceptionally high ΔE^*_{vis} values. These molecules are the fluorocarbons and the highly symmetrical molecules such as neo-pentane, cyclohexane, CCl_4, and benzene. These results suggest that the mechanism for viscous flow involves an additional rotational energy requirement not found in molecules with central force fields. On the basis of collision theory for momentum transfer, both translational and rotational energy of molecules may be exchanged. Rotational energy exchange and translational-rotational exchange will be of significant magnitude only if the force fields of a pair of interacting molecules (or at least one of the pair) are acentric. The force fields of unbranched hydrocarbons are quite central while those of the fluorocarbons, CCl_4, neo-pentane, benzene, etc., are acentric.

Corresponding States for Binary Mixtures. In a series of papers [11, 12, 9, 10, 89], Boon, Thomaes et al., have measured relative viscosities of simple molecules (Ar, Kr, Xe, CH_4, CD_4 and O_2) and suggested a reduced relationship for such molecules and their mixtures obtained in a manner similar to equation 38.

These authors propose that

$$\ln \mu = a + \frac{b}{T} , \tag{43}$$

be reduced to

$$\mu_r = \mu/Z \tag{44}$$

where

$$Z = (E^* \; r^{*2}/m)^{1/2} \tag{45}$$

and μ_r is a universal function of T_r, where

$$T_r = kT/E^* . \tag{46}$$

Substituting 44 into 43 and differentiating with respect to 1/T implies that

$$\frac{b}{T} = \frac{b_r}{T_r} , \tag{47}$$

where b_r is a universal constant. Then from equations 43, 44, and 47,

$$\ln \mu_r = a - \ln Z + \frac{b_r}{T_r} \tag{48}$$

and

$$a - \ln Z = \text{constant for all substances.} \tag{49}$$

By equations 36, 37, and 45

$$a = \ln [(BM)^{1/2}/A^{1/3}] + \text{constant.} \tag{50}$$

A plot of "a" (obtained from μ values extrapolated to $1/T = 0$) versus $(EM)^{1/2}/A^{1/3}$ was constructed with a line of unit slope drawn to give the best fit to the Ar, Kr, Xe, and CH_4 points (Figure 33).

From equations 46, 47, and 37

$$b = \frac{b_r}{k} E^* = (\text{constant}) \left(\frac{A}{B}\right). \tag{51}$$

A plot of "b" (obtained from $\partial \ln \mu/\partial(1/T)$) versus $\left(\frac{A}{B}\right)$ was constructed and the best straight line was drawn from the origin through the Ar, Kr, Xe, and CH_4 points (Figure 34).

From knowledge of A and B, Figures 33 and 34 should give the a and b values, respectively, which permit calculation of the viscosities for the simple molecules by equation 43.

Prigogine [75] has shown that for his average potential model, the average values $\langle E^* \rangle$ and $\langle r^* \rangle$, for the species in a binary mixture are given by

$$\langle E^* \rangle = \frac{\left[X_1^2 E_1^* r_1^{*6} + 2X_1 X_2 E_{12}^* r_{12}^{*6} + X_2^2 E_2^* r_2^{*6}\right]^{n/(n-6)}}{\left[X_1^2 E_1^* r_1^{*n} + 2X_1 X_2 E_{12}^* r_{12}^{*n} + X_2^2 E_2^* r_2^{*n}\right]^{6/(n-6)}} \tag{52}$$

$$\langle r^* \rangle = \left[\frac{X_1^2 E_1^* r_1^{*n} + 2X_1 X_2 E_{12}^* r_{12}^{*n} + X_2^2 E_2^* r_2^{*n}}{X_1^2 E_1^* r_1^{*6} + 2X_1 X_2 E_{12}^* r_{12}^{*6} + X_2^2 E_2^* r_2^{*6}}\right]^{1/(n-6)} \tag{53}$$

for the Lennard-Jones (6-n) potential. Subscripts 1 and 2 imply interactions between pairs of like molecules and subscript 12 implies

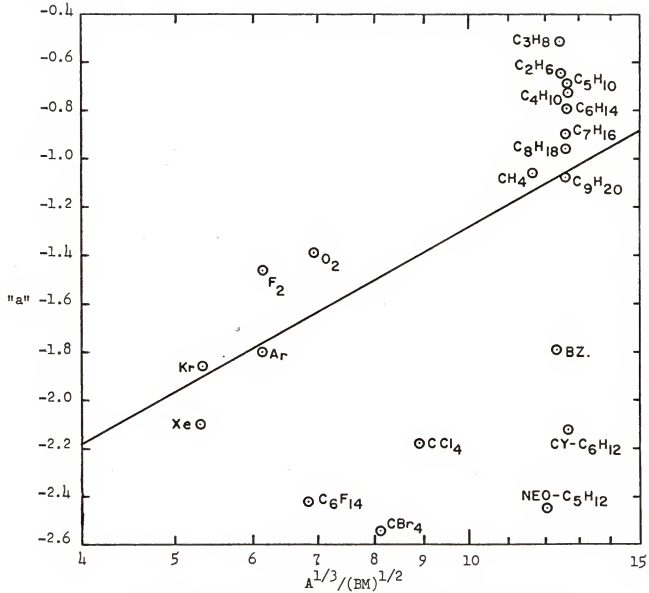

Figure 33.--Reduced Relationship for "a" of Equation 43

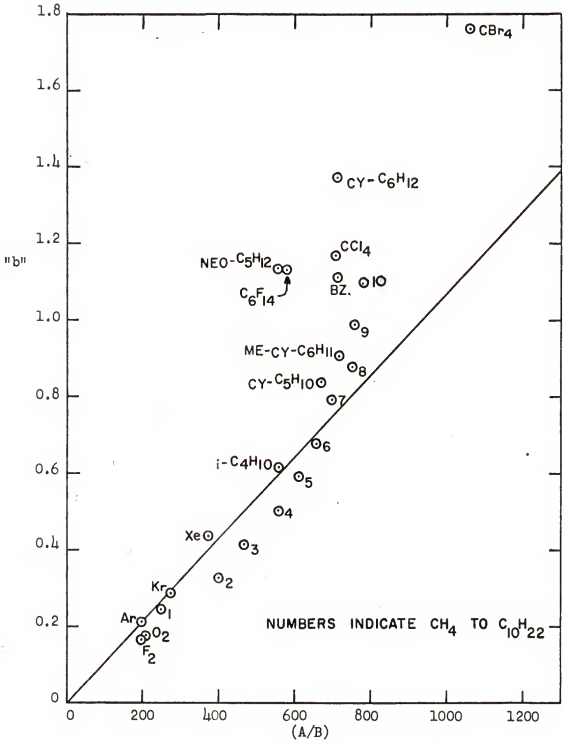

Figure 34.--Reduced Relationship for "b" of Equation 43

pair-interactions between unlike species. Assuming the usual combining rules,

$$E^*_{12} = (E^*_1)^{1/2} \, (E^*_2)^{1/2} \tag{54}$$

and

$$r^*_{12} = (r^*_1 + r^*_2)/2 \; . \tag{55}$$

Equations 52 and 53 were written in terms of A and B by equations 36 and 37 and values of $\left\langle \frac{A}{B} \right\rangle_{12}$ and $\left\langle \frac{(BM)^{1/2}}{A^{1/3}} \right\rangle_{12}$ were calculated for the various mixtures of simple molecules. Values of a and b from Figures 33 and 34 then gave $\mu_{calc.}$ for these mixtures which could be compared with the experimental values.

The calculated values for the Ar - Kr system were in excellent agreement with experiment. μ versus composition shows a minimum of approximately 0.8 millistokes [9] below a linear function and the calculated values are within 0.05 millistokes of the experimental value of 1.88 millistokes.

Experimental kinematic viscosities for the Ar - CH_4 and Kr - CH_4 systems (2.76 and 1.68 millistokes, respectively [11]) represent negative deviations of 1.1 and 1.2 millistokes below linear μ versus mole fraction relationships. The calculated values predicted positive deviations of 0.5 and 0.2 millistokes above the linear relationship, respectively.

The O_2 - Ar system exhibits only very slight positive deviations in μ from linearity. The experimental value of 1.96 millistokes [28]

represents a deviation of only +0.05 millistokes while the calculated value predicts a positive deviation of +0.9 millistokes.

For the above systems of simple molecules, other than Ar - Kr, the predicted values are definitely too high. For the benzene - CCl_4 and benzene - cyclohexane systems (μ = 5.967 ms. and 7.344 ms., respectively [33, 19]) the calculations gave values which were too low (deviations of -2.7 and -4.7 millistokes compared to deviations of -0.4 and -1.6 millistokes experimentally).

Lennard-Jones (m-n) values for the above compounds have been estimated [79] to be (6-12) for Ar, Kr, and CH_4, (6-17) for O_2, and (7-28) for benzene, CCl_4 and cyclohexane. Changing equations 52 and 53 to fit a (7-28) potential function did not noticeably alter the calculated kinematic viscosity for the benzene - CCl_4 system. This indicates that the form of the potential function is probably not the primary source of disagreement between the theory and experiment.

The primary source of disagreement is probably to be found in the assumption that only the configurational space part of the partition function and not the momentum space part is important in establishing the corresponding states treatment of transport properties. Another defect might also be in the use of the average potential model for mixtures.

VII. CONCLUSIONS

Liquid viscosities can not be explained, or indeed even correlated by any of the theories thus far proposed. Any adequate theory will apparently have to include terms involving energies of rotational interaction [74, 63, 43, 44] (most noticeable for the molecules with acentric force fields such as the fluorocarbons and the quasi-spherical hydrocarbons). This suggestion is supported by the larger increases in the temperature coefficient of viscosity with branching for the smaller hydrocarbons (e.g., n-C_5H_{12}, and neo-C_5H_{12}) as compared to the absence of this increase with branching for the larger hydrocarbons in which the chains can coil (e.g., the isomeric C_8H_{18} compounds in Table 16). Other evidence lies in the fact that CBr_4, with its extremely acentric force field, exhibits the highest temperature coefficient of viscosity of any of the 52 molecules tested. Further, Andrade and Dodd [3] have found that for polar liquids an electrical field applied in the direction of flow has little effect on the viscosity whereas a transverse field produces a marked increase in viscosity. This last observation may be explained as an additional rotational interaction when the molecules are either aligned perpendicular to the direction of flow or have formed clusters about ions [3]. A field applied in the direction of flow would be expected to have little influence on the viscosity as the molecules would tend to align in the direction of flow and thus not increase any rotational interaction. Finally, the only mixtures

for which the corresponding states treatment predicted correct values of the viscosity were those in which the molecules, Ar and Kr, have truly central force fields.

The fact that corresponding states treatments, even for conformal systems, gave results which deviated further from experiment than did a simple linear relation for μ in terms of mole fraction indicates that the use of the configurational partition function is inadequate. It appears that the momentum integral must be included to account for rotational and translational-rotational energy exchanges. The correctness of the reducing parameters, A and B, used in this work is shown by the fact that they effectively correlate other properties (including gas viscosities [6]) for these molecules. The idea that the primary difficulty lies in the partition function, rather than in the potential used, is further supported by the fact that Lennard-Jones (6-12) and (7-28) potentials gave essentially identical values for $\mu_{calc.}$. Similarly, a Sutherland potential applied [39] to the theory of Born and Green [13] gave results which were at least as good as a Lennard-Jones (6-12) potential. It is obvious that a Sutherland potential contains an unrealistic repulsive potential. While the repulsive portion of the pair potential is probably the most important in liquid viscosities, correlations with the attractive portion [35, 34, 83] should not be overlooked.

Structural changes that accompany temperature changes [64, 35] in the pure liquids and that accompany both composition and temperature changes in mixtures (Class 3 solutions in Chapter V) must be incorporated

in any new theory. Eyring's extension of his theory to include such structural changes [68] is quite inadequate in that it is based upon hypothetical deviations from equation 22 which are opposite in direction and of a different form from those actually observed [1, 46, 92]. Low angle X-ray studies [14] are in agreement with the structural changes proposed in Chapter V for system ten.

Future viscosity studies should include the fluorocarbons because comparison of these compounds with hydrocarbons and other materials clearly shows the inadequacies of the various theories. Viscosities of symmetrical molecules with extremely short liquid ranges should be studied (e.g., 2,2,3,3-tetramethylbutane and acetylene).

The forms of the curves for the surface tensions of mixtures as a function of composition should be further investigated as well as the interesting observation of the rising of certain liquids on glass walls discussed in Chapter IV.

BIBLIOGRAPHY

1. American Petroleum Institute Research Project 44, Carnegie Institute of Technology, "Selected Values of Physical Properties of Hydrocarbons and Related Compounds."

2. Andrade, E. N. Da C., "Viscosity and Plasticity," Chemical Publishing Co., New York, 1951.

3. Andrade, E. N. Da C., and Dodd, C., Proc. Roy. Soc., A187, 298 (1946).

4. Askew, W. C., Ph.D. Dissertation, University of Florida, 1966.

5. ASTM Designation: D445-53T.

6. Bae, J. H., Ph.D. Dissertation, University of Florida, 1966.

7. Birch, F., Phys. Rev., 41, 641 (1952).

8. Blomgren, G. E., Ann. N.Y. Acad. of Sci., 79, 781 (1960).

9. Boon, J. P., and Thomaes, G., Physica, 28, 1074 (1962).

10. Boon, J. P., and Thomaes, G., Physica, 28, 1197 (1962).

11. Boon, J. P., and Thomaes, G., Physica, 29, 123 (1963).

12. Boon, J. P., and Thomaes, G., Physica, 29, 208 (1963).

13. Born, M., and Green, H. S., "A General Kinetic Theory of Liquids," Cambridge University Press, New York, 1949.

14. Brady, G. W., J. Chem. Phys., 32, 45 (1960).

15. Brush, S. G , Chem. Rev., 62, 513 (1962).

16. Carmichael, L. T., J. Chem. Eng. Data, 10, 57 (1965).

17. Cecil, R. R., and Reed, T. M., III, Unpublished data.

18. Cohen, M. H., and Turnbull, D., J. Chem. Phys., 31, 1164 (1959).

19. Collins, D. A., and Watts, H., Aust. J. Chem., 17, 516 (1964).

20. Collins, Frank C., and Raffel, Helen, The Hournal of Chem. Phys., 29, 699 (1958).

21. Cook, G. A. (ed.), "Argon, Helium, and the Rare Gases," vols. 1 and 2, Interscience Publishers, New York, 1961.

22. Dahler, J. S., and Hirschfelder, J. O., J. Chem. Phys., 32, 330 (1960).

23. Din, F., "Thermodynamic Functions of Gases," vols. 2 and 3, Butterworths, London, 1962.

24. Doolittle, A. K. and Doolittle, D. B., Journal of Applied Phys., 28, 901 (1957).

25. Dow Chemical Co., "Physical Properties of Chemical Substances," Midland, Michigan.

26. Dow, R. B., Phil. Mag., 28, 403 (1939).

27. Driesbach, R. R., "Physical Properties of Chemical Compounds," American Chemical Society, Washington, 1955.

28. Fontaine-Limbourg, M. C., Legros, J. C , Bonn, J. P., and Thomaes, G., Physica, 31, 396 (1965).

29. Freyer, E. B., Hubbard, J. C., and Andrews, D. H., J. Am. Chem. Soc., 51, 758 (1929).

30. Friend, J. N., and Hargreaves, W. D., Phil. Mag., 34, 643 (1943).

31. Geist, J. M., and Cannon, M. R., Ind. Eng. Chem., Anal. Ed., 18, 611 (1946).

32. Glasstone, S., Laidler, K. J., and Eyring, H., "The Theory of Rate Processes," McGraw Hill Book Co., New York, 1941.

33. Grunberg, L., Trans. Far. Soc., 50, 1293 (1954).

34. Grunberg, L., and Nissan, A. H., Nature, 154, 146 (1944).

35. Grunberg, L., and Nissan, A. H., Trans. Far. Soc., 45, 125 (1949).

36. Grunberg, L., and Nissan, A. H., Nature, 164, 799 (1949).

37. Hammond, L. W. et al., J. Phys. Chem., 62, 637 (1958).

38. Heiks, J. R., and Orban, E., J. Phys. Chem., 60, 1065 (1956).

39. Higgins, T. H. S., and Raw, C. J. G., J. Chem. Phys., 27, 623 (1957).

40. Hildebrand, J. H., Fisher, B. B., and Benesi, H. A., J. Am. Chem. Soc., 72, 4348 (1950).

41. Hildebrand, J. H., and Scott, R. L., "Solubility of Nonelectrolytes," 3rd ed., Reinhold Publishing Corp., New York, 1950.

42. Hildebrand, J. H., and Scott, R. L., "Regular Solutions," Prentice-Hall, Inc., Englewood Cliffs, N.J., 1962.

43. Hill, N. E., Proc. Phys. Soc., 67-B, 149 (1954).

44. Hill, N. E., Proc. Roy. Soc., A240, 101 (1957).

45. Innes, K. K., J. Phys. Chem., 66, 817 (1956).

46. International Critical Tables, McGraw-Hill Book Co., Inc., New York, 1933.

47. Jacobson, B., and Laurent, T., Acta Chem. Scand., 7, 58 (1953).

48. Jaeger, F. M., "Second Report on Viscosity and Plasticity," N. V. Noord-Hollandsche Uitgevers-maatschappij, Amsterdam, 1938.

49. Jobling, A., and Lawrence, A. S. C., Proc. Roy. Soc., A206, 257 (1951).

50. Jobling, A., and Lawrence, A. S. C., J. Chem. Phys., 20, 1296 (1952).

51. Jones, G., and Ray, W. A., J. Am. Chem. Soc., 59, 187 (1937).

52. Jura, G., Fraga, D., Mika, G., and Hildebrand, J. H., Proc. Nat'l. Acad. Sci., 39, 19 (1953).

53. Kampmeyer, P. M., J. of Applied Phys., 23, 99 (1951).

54. Kobe, A. K., and Lynn, R. E., Jr., Chem. Rev. 52, 117 (1953).

55. Landolt-Börnstein, "Physikalish-Chemische Tabellen," J. Springer, Berlin, 1923.

56. Legros, J. C., and Thomaes, G., Physica, 31, 703 (1965).

57. Lipkin, M. R. et al., Ind. Eng. Chem., Anal. ed., 16, 55 (1944).

58. Lowry, B. A., Rice, S. A., and Gray, P., J. Chem. Phys., 40, 3673 (1964).

59. Macedo, P. B., and Litovitz, T. A., J. Chem. Phys., 42, 245 (1965).

60. Majumdar, D. K., J. Phys. Chem., 67, 1374 (1963).

61. Mathias, E., Crommelin, C. A., and Meihuizen, J. J., Physica, 4, 1200 (1937).

62. McLaughlin, E., Trans. Far. Soc., 55, 28 (1959).

63. McLaughlin, E., Physica, 26, 650 (1960).

64. McLaughlin, E., and Ubbelohde, A. R., Trans. Far. Soc., 54, 1804 (1958).

65. Miller, A. A., J. Phys. Chem., 67, 1031 (1963).

66. Minnesota Mining and Manufacturing Co., communication.

67. Moelwyn-Hughes, E. A., "Physical Chemistry," 2nd ed., Macmillan, New York, 1961.

68. Moore, R. J., Gibbs, Peter, and Eyring, Henry, J. Phys. Chem., 57, 172 (1953).

69. Mueller, C., and Lewis, J., J. Chem. Phys., 26, 286 (1957).

70. Mumford, S. A., and Phillips, J. W. C., J. Chem. Soc., 1950, 75.

71. Partington, J. R., "An Advanced Treatise on Physical Chemistry," vol. 2, Longmans, Green & Co., New York, 1951.

72. Perry, J. H. (ed.), "Chemical Engineers Handbook," 3rd ed., McGraw-Hill Book Co., Inc., New York, 1950.

73. Phibbs, M. K., J. Chem. Phys., 19, 1420 (1951).

74. Pople, J. A., Physica, 19, 668 (1953).

75. Prigogine, I., Bellemans, A., and Mathot, V., "The Molecular Theory of Solutions," Interscience Publishers, New York, 1957.

76. Reed, T. M., III, J. Phys. Chem., 59, 425 (1955).

77. Reed, T. M., III, Anal. Chem., 30, 221 (1958).

78. Reed, T. M., III, "Fluorine Chemistry," vol. 5, J. H. Simons (ed.), Academic Press, New York, 1963.

79. Reed, T. M., III, and McKinley, M. D., J. Chem. and Eng. Data, 9, 553 (1965).

80. Reed, T. M., III, and Taylor, T. E., J. Phys. Chem., 63, 58 (1959).

81. Reynolds, O., Phil. Trans., 177, 157 (1886).

82. Rowlinson, J. S., "Liquids and Liquid Mixtures," Academic Press, New York, 1959.

83. Simons, J. H., and Wilson, W. H., J. Chem. Phys., 23, 613 (1955).

84. Smith, E. B., and Hildebrand, J. H., J. Chem. Phys., 31, 145 (1959).

85. Starling, K. E. et al., A. I. Ch. E. Journal, 6, 438 (1960).

86. Swift, B. W., Lohrenz, J., and Kurcta, F., A. I. Ch. E. Journal, 6, 415 (1960).

87 Telang, M. S., J. Phys. Chem., 49, 579 (1945).

88. Telang, M. S., J. Phys. Chem., 50, 373 (1946).

89. Thomaes, G., and Van Itterbeek, J., Molecular Phys., 2, 372 (1959).

90. Thomas, L. H., J. Chem. Soc., 1946, 573.

91. Thomas, L. H., J. Chem. Soc., 1947, 822.

92. Timmermans, J., "Physico-Chemical Constants of Pure Organic Compounds," Elsevier, Amsterdam, 1950.

93. Weissberger, A. (ed.), "Physical Methods of Organic Chemistry," vol. 1, pp. 167-172, Interscience Publishers, Inc., New York, 1945.

94. Weymann, H. D., Kolloid Z., 181, 131 (1962).

95. Wood, S. E., and Austin, A. E., J. Am. Chem. Soc., 67, 480 (1945).

96. Wood, Scott E., and Gray, J. A., III, J. Am. Chem. Soc., 74, 3733 (1952).

97. Yen, L. C., M.S. Thesis, University of Florida, 1957.

98. Yen, L. C., and Reed, T. M., III, J. Chem. and Eng. Data, 4, 102 (1959).

BIOGRAPHICAL SKETCH

Thomas Elliott Taylor was born July 9, 1931, at Ross, California. In June, 1949, he graduated from Biglerville High School, Biglerville, Pennsylvania. From June, 1949, through August, 1956, he worked at the Petroleum Refining Laboratory of The Pennsylvania State University. He received the degrees of Bachelor of Science in January, 1954, and Master of Science in June, 1956, from that University. In 1956, he enrolled in the Graduate School of the University of Florida. He worked as a research associate until 1960, as teaching assistant until 1961, and as interim instructor until 1962. From 1962 until 1964, he was assistant professor of chemistry at George Peabody College in Nashville, Tennessee. He served as an Associate Scientist in the Special Training Division of the Oak Ridge Institute for Nuclear Studies from 1964 until 1965. In September, 1965, he returned to the University of Florida as a National Science Foundation, Science Faculty Fellow. From that time until the present he has pursued his work toward the degree of Doctor of Philosophy.

Thomas Elliott Taylor is married to the former Sandra Beckett and they are the parents of nine children. He is a member of the American Chemical Society, in which he has served as a member of the Curriculum Committee in the Division of Chemical Education, and a member of Phi Lambda Upsilon, Gamma Sigma Epsilon, and Sigma Xi. He was a DuPont Teaching Fellow in 1961-62.

This dissertation was prepared under the direction of the chairman of the candidate's supervisory committee and has been approved by all members of that committee. It was submitted to the Dean of the College of Arts and Sciences and to the Graduate Council, and was approved as partial fulfillment of the requirements for the degree of Doctor of Philosophy.

April, 1967

Dean, College of Arts and Sciences

Dean, Graduate School

Supervisory Committee:

Co-Chairman

Co-Chairman